



HAL
open science

Trophic ecology of a blooming jellyfish (*Aurelia coerulea*) in a Mediterranean coastal lagoon

Raquel Marques, Delphine Bonnet, Claire Carré, Cécile Roques, Audrey M. Darnaude

► **To cite this version:**

Raquel Marques, Delphine Bonnet, Claire Carré, Cécile Roques, Audrey M. Darnaude. Trophic ecology of a blooming jellyfish (*Aurelia coerulea*) in a Mediterranean coastal lagoon. *Limnology and Oceanography*, 2021, 66 (1), pp.141-157. 10.1002/lno.11593 . hal-03411044

HAL Id: hal-03411044

<https://hal.umontpellier.fr/hal-03411044v1>

Submitted on 17 Nov 2021

HAL is a multi-disciplinary open access archive for the deposit and dissemination of scientific research documents, whether they are published or not. The documents may come from teaching and research institutions in France or abroad, or from public or private research centers.

L'archive ouverte pluridisciplinaire **HAL**, est destinée au dépôt et à la diffusion de documents scientifiques de niveau recherche, publiés ou non, émanant des établissements d'enseignement et de recherche français ou étrangers, des laboratoires publics ou privés.

1 **Trophic ecology of a blooming jellyfish (*Aurelia coerulea*) in a**
2 **Mediterranean coastal lagoon**

3
4 *Raquel MARQUES¹, Delphine BONNET¹, Claire CARRÉ¹, Cécile ROQUES¹, Audrey M.*
5 *DARNAUDE¹*

6 ¹ MARBEC, Univ. Montpellier, CNRS, Ifremer, IRD, Montpellier, France

7
8
9 **Corresponding author:**

10 marques.rfs@gmail.com / raquel.marques@umontpellier.fr

11 CC093, Place Eugène Bataillon, 34095 Montpellier Cedex 05, France

12 Tel: +33769370312

13 **Co-authors contact:**

14 delphine.bonnet@umontpellier.fr; claire.carre@ird.fr; Cecile.Roques@cnrs.fr;

15 Audrey.Darnaude@cnrs.fr

16
17 **Running head:** Trophic ecology of jellyfish in a coastal lagoon

18 **Key words:** Stable Isotopes, Diet, Trophic niche, Trophic competition, Population dynamics,

19 Scyphistomae, Medusae, Oysters

20 **Abstract**

21 The current lack of knowledge on the trophic ecology of scyphozoans, particularly at the
22 benthic stage, prevents a full understanding of the controls on many jellyfish blooms. The
23 blooming scyphozoan (*Aurelia coerulea*) completes its entire life cycle in the Thau lagoon
24 (southern France), where the annual population dynamics of both its benthic and pelagic
25 stages have been described. This offered an exceptional framework to investigate the trophic
26 processes regulating jellyfish populations over time. To this aim, stable isotopic signature
27 analysis ($\delta^{13}\text{C}$ and $\delta^{15}\text{N}$) was used to infer the diet of both *A. coerulea* scyphistomae and
28 medusae over one year. These results were matched with medusae gut content analysis and
29 with the monthly abundances of local plankton groups. Lastly, the isotopic signatures of *A.*
30 *coerulea* scyphistomae and medusae were compared with those of the oysters (*Crassostrea*
31 *gigas*) cultivated in the lagoon to evaluate the potential interspecific trophic competition. The
32 results revealed two seasonal shifts in the trophic niche of *A. coerulea* and substantial overlap
33 between the diets of its benthic and pelagic stages. Conversely, trophic niche overlaps with
34 the oysters were restricted, suggesting a limited impact of the local jellyfish bloom on
35 shellfish production. Phytoplankton, microzooplankton, mesozooplankton, and sedimentary
36 organic matter were all important food sources during critical periods of *A. coerulea* life-
37 cycle. However, microzooplankton abundance was found to be key for the production of
38 buds by the scyphistomae and, therefore it is likely to control the benthic population size and,
39 thereby, to modulate the intensity of its annual bloom in Thau.

40 **Introduction**

41 Due to the impact of their conspicuous blooms on coastal ecosystems functioning and
42 economic activities, jellyfish have received increasing scientific attention during the last
43 decades (Purcell 2012). In particular, the ecological drivers of jellyfish mass occurrences
44 have been investigated, revealing a complex interaction of natural (e.g. Condon et al. 2012)
45 and anthropogenic (e.g. Purcell 2012) causes. However, uncovering the drivers of blooms is
46 particularly challenging for most scyphozoan blooming species because their life-cycle
47 comprises a benthic (scyphistomae) and a pelagic (ephyrae and medusae) phase (e.g. Lucas
48 2001). Therefore, bloom formation is a joint consequence of the production of pelagic
49 ephyrae by the benthic scyphistomae and of their survival and growth into medusae. As a
50 result, the ecology of both life stages controls bloom intensity.

51 Bottom-up processes within food webs often play a key role in ecological systems functioning
52 and are amongst the most important drivers of jellyfish blooms (Boero et al. 2008). Food
53 quality and availability are known to control the production of ephyrae by the scyphistomae
54 (Han and Uye 2010; Ikeda et al. 2017) and to modulate the growth rate of medusae (Ishii and
55 Båmstedt 1998). This supports the need for comprehensive studies on the trophic ecology of
56 both life stages in the field. Yet, although information is growing on the trophic ecology of
57 medusae (e.g. Javidpour et al. 2016; Milisenda et al. 2018), the diet of jellyfish scyphistomae
58 is still poorly known.

59 Jellyfish from the *Aurelia* genus are present globally in coastal areas and are among the most
60 common scyphozoans that form blooms (Mills 2001). Large accumulations of *Aurelia* spp.
61 have been reported all around the world, including in the Mediterranean, where they occur
62 mainly in protected waters and semi-enclosed seas (Mills 2001). Their medusae have been
63 described as zooplanktivorous, with a dominance of mesozooplankton, especially copepods,
64 in their diet (e.g. Ishii and Tanaka 2001; Lo and Chen 2008). However, while

65 microzooplankton and benthic food sources have been considered for long as negligible food
66 sources for jellyfish, recent findings based on new techniques (such as stable isotope analysis)
67 suggest the opposite (Javidpour et al. 2016). In laboratory studies, newly hatched *Artemia* sp.
68 are usually provided as food (e.g. Han and Uye 2010, Hubot et al. 2017), but the few studies
69 regarding the diet of *Aurelia* sp. scyphistomae in the wild suggest that they eat a mix of
70 phytoplankton (Huang et al. 2015), microzooplankton (Kamiyama 2013) and small
71 mesozooplankton species (e.g. copepods, cladocerans, gelatinous zooplankton; Östman 1997).
72 Considering the critical role of scyphistomae in the formation of scyphozoans blooms, it is
73 urgent to specify natural prey preferences in *Aurelia* species and the potential trophic
74 competition among their benthic and pelagic stages to understand blooms formation in this
75 genus and evaluate their ecological consequences.

76 Situated along the North-western Mediterranean coast, the Thau lagoon offered an
77 exceptional framework for this. Indeed, this lagoon presents the rare particularity to harbour a
78 complete resident population of *Aurelia coerulea* (Bonnet et al. 2012; Marques et al. 2015a),
79 which allows investigating the trophic processes that regulate its population dynamics at both
80 stages. The scyphistomae of *A. coerulea* are widespread in the lagoon, fixed mainly on
81 biofouling organisms that grow on anthropogenic structures (predominantly on oysters and
82 mussels; Marques et al. 2015a). They are present all year round, with a peak of coverage in
83 the Spring (April) and lower densities in the Summer and Autumn (Marques et al. 2019).
84 Ephyrae appear in the early winter (November – December) and give rise to adult medusae at
85 the beginning of the Spring (April – May), generating the annual jellyfish bloom, which
86 persists until June – July (Bonnet et al. 2012; Marques et al. 2015b). Because no clear link
87 was found between the abundance of mesozooplankton in the lagoon and the benthic
88 population dynamics of *A. coerulea*, it was suggested that other food sources might sustain

89 the species local production (Marques et al. 2019). Nevertheless, further confirmation is still
90 required in this regard.

91 Coastal lagoons are usually very productive environments, where high continental inputs in
92 nutrients and particulate organic matter sustain high and diversified primary and secondary
93 productions (Nixon et al. 1995). This benefits the whole food web and enhances the growth of
94 lagoon predators like juvenile fish (Escalas et al. 2015). In Thau, it also supports a massive
95 shellfish production: ~10% of the Pacific oysters *Crassostrea gigas* produced in France come
96 from the lagoon, with a yearly shellfish production of 15 000 tons (Mongruel et al. 2013).

97 In this context, the present work not only aimed to describe the trophic ecology of both the
98 benthic and the pelagic life-stages of *A. coerulea* in Thau and assess its influence on critical
99 periods of population dynamics of this jellyfish (e.g. peak of bud production, strobilation, and
100 medusae growth), but also to evaluate whether *A. coerulea* medusae and scyphistomae
101 compete for food with the Pacific oysters reared in the lagoon. For this, we combined
102 medusae gut content assessments with stable isotopes analysis. This latter technique has been
103 increasingly used to study the structure and transfer of organic matter within coastal food
104 webs (Layman et al. 2012) and has recently allowed uncovering the diet, trophic levels, and
105 trophic interactions of different jellyfish species (Fleming et al. 2015; Javidpour et al. 2016;
106 Milisenda et al. 2018). Using it to explore the changes in *A. coerulea* diet during a full annual
107 cycle should allow assessing whether its benthic and pelagic stages occupy the same trophic
108 niche than the oysters cultivated in the lagoon. This strongly contributes to a better
109 understanding of the impacts of *A. coerulea* blooms on the local shellfish production.

110

111 **Material and Methods**

112 *Study site*

113 The Thau lagoon is a semi-enclosed marine coastal lagoon of 75 km² area, connected
114 to the Mediterranean Sea by three narrow channels (Fig. 1). It is relatively shallow, with mean
115 and maximum depths of 4 and 10 m, respectively (except for a localized depression of 24 m).
116 The local tidal range (< 1m) is weak, so water residence time in the lagoon is globally high
117 (1–4 months) and strongly influenced by seasonal strong wind events (Millet and Cecchi
118 1992). The lagoon environment parameters show strong seasonal variations, characteristic of
119 temperate regions, with temperature and salinity at their lowest in the winter (with minimum
120 values of 7.6 and 35.0, respectively) and at their highest in the summer (with maximum
121 values of 25.8 °C and 39.6, respectively; Marques et al 2019). The lagoon mainly receives
122 water from the Sète canal that connects it to the Mediterranean Sea and from several small
123 intermittent rivers that drain its catchment area (290 km², Plus et al. 2006). These later dry out
124 between May and September and show occasional flash floods in the wet season (Fouilland et
125 al. 2012). As a result, marine conditions prevail in the lagoon, the annual influence of the
126 freshwater coming from the watershed being highly dependent on the intensity of rainfall
127 events during the winter (Plus et al. 2006). With regards to anthropogenic influence, the
128 lagoon is under multiple pressures due to the presence of the touristic city of Sète and many
129 small villages and agriculture fields on its coastline. Shellfish farming is the most important
130 economic activity on the lagoon (Mongruel et al. 2013): around 20% of its surface is occupied
131 by farms, mainly in the northern and north-western parts (Fig. 1).

132

133 *Sampling*

134 For this study, the jellyfish and their potential food sources were sampled in the
135 eastern part of the lagoon, at two close sites where the benthic and the pelagic population
136 dynamics of *A. coerulea* had been previously described (Bonnet et al. 2012; Marques et al.
137 2015b; Marques et al. 2019). Both sites (benthic sampling site: 43°25'31.1"N; 03°42'0.9"E

138 and pelagic sampling site: 43°23'59.1''N; 03°36'37.2''E; Fig. 1) are located on soft-bottom
139 sediments punctuated by sparse seagrass meadows and are strongly influenced by marine
140 water influxes due to their proximity to the Sète channel, which connects the lagoon to the
141 Mediterranean Sea.

142 *A. coerulea* scyphistomae were collected monthly on a partially submerged boat present at
143 the benthic sampling site (see Marques et al. 2019 for more details), over an entire calendar
144 year (from January 2017 to January 2018). For this, mussel shells with sizeable aggregates of
145 scyphistomae attached on their underside surface (three per sampling date) were collected
146 directly on the surface of the boat by SCUBA diving. They were brought to the laboratory in
147 ambient water and placed in 0.2- μ m-filtered seawater (ca. 20°C) for about 2h to ensure all
148 scyphistomae had empty guts. Fifty individual scyphistomae were then collected under a
149 dissecting microscope (Olympus SZ40; Olympus KL 1500 LCD), using needles and tweezers
150 to carefully detach them, and preserved in cryotubes at -30°C.

151 The pelagic ephyrae of *A. coerulea* are usually present in the lagoon from November to April
152 (Bonnet et al. 2012; Marques et al. 2015b). However, because stable isotope analysis requires
153 pooling high numbers of these small organisms to be applicable, sampling for this life stage in
154 this work was successful in January 2018 only. The ephyrae were collected near the water
155 surface at the pelagic sampling site, by horizontal towing, using a modified WP2 plankton net
156 (1.2 m long, 50-cm opening, and 200- μ m mesh). In the laboratory, they were picked and kept
157 for ca. 2h in filtered seawater to allow for complete gut evacuation. Then 50 individuals were
158 pooled per sample and preserved at -30°C.

159 *A. coerulea* medusae (i.e., pelagic individuals with bell diameter > 1 cm), were collected
160 every two weeks at the pelagic sampling site, from March to June 2017, i.e., over the entire
161 period of their presence in the lagoon. They were collected in surface waters using hand nets
162 and transported to the laboratory in ambient water. Five individual medusae were then

163 randomly selected and prepared for stomach content analysis. For this, they were each
164 partially dried on a paper towel to remove excess water, measured (bell diameter in cm),
165 weighted (total wet weight in g), and individually preserved in 4% buffered formaldehyde.
166 The remaining medusae were kept for ca. 2h in 0.2 μm filtered seawater (ca. 20°C) to empty
167 their guts. Three of them were then placed on a paper towel for about 1 minute (30 s on each
168 side) to remove excess water, weighed, and measured. As bell tissue is the most suitable body
169 part for stable isotope analysis in jellyfish (D'Ambra et al. 2014), gonads, oral arms, and
170 gastric pouches were removed from each medusa. The remaining individual bell tissues were
171 preserved separately at -30°C. In March 2017, due to the small size of the medusae (ca. 2 cm
172 bell diameter), eight complete individuals were pooled per replicate before preservation at -
173 30°C.

174 For this work both the plankton and the sedimentary organic matter of the lagoon were also
175 sampled as they both constitute potential food sources for *A. coerulea*. Samples for these two
176 components were collected at pelagic and benthic sampling sites, respectively, on the same
177 sampling dates as *A. coerulea* medusae and scyphistomae collection. Within the plankton, the
178 fraction larger than 200 μm , that between 60 and 200 μm and that between 20 and 60 μm
179 were assumed to be composed mainly by mesozooplankton, microzooplankton, and
180 phytoplankton, respectively. Mesozooplankton samples were collected near the surface, by
181 horizontal towing, using a modified WP2 plankton net (length: 1.2 m; opening area: 50 cm;
182 mesh size: 200 μm). Once in the laboratory, each sample was filtered through a 60 μm mesh
183 sieve to eliminate excess water and divided into five subsamples. Microzooplankton and
184 phytoplankton samples were also collected by horizontal towing near the surface, but using a
185 phytoplankton net (length: 1 m; opening area: 30 cm; mesh size: 20 μm). Once in the
186 laboratory, each sample was filtered through a 200- μm sieve. The size fraction $> 200 \mu\text{m}$ was
187 discarded. The remaining sample was then separated into the two size fractions,

188 corresponding to microzooplankton and phytoplankton, using a 60 μm sieve, and then divided
189 into 5 subsamples. For each plankton size fraction, the subsamples were collected separately
190 on pre-combusted (500°C for 24h) Whatman GF/F filters. Two filters of each plankton
191 component were acidified with 1% HCl and triple rinsed with distilled water to remove
192 inorganic carbon, which can bias C stable isotope results (Yokoyama et al. 2005). The
193 remaining non-acidified filters were used for N stable isotope analysis, since sample
194 acidification may affect the stable isotope signature for this element (Pinnegar and Polunin
195 1999). All samples were preserved at -30°C until further analysis. For sedimentary organic
196 matter, the first 2 cm of the sediment were collected by SCUBA diving at the benthic
197 monitoring site. Samples (2 replicates) were carefully scrutinized to eliminate any large
198 organisms, sediment inorganic particles, or vegetal debris, before preservation at -30°C .
199 To investigate the trophic interactions between *A. coerulea* and the local oysters, both wild
200 and cultivated individuals of *Crassostrea gigas* were sampled seasonally from October 2017
201 to August 2018, including during the peak of the jellyfish bloom (which occurred in June in
202 2018). Wild oysters (mean size: 11.5 ± 2.0 cm) were collected by SCUBA diving at the
203 benthic monitoring site, while the cultivated ones (mean size: 11.9 ± 1.0 cm) were obtained
204 from the shellfish producer *Huitres-Bouzigues.com*. Immediately after their removal from the
205 lagoon, the oysters were transported to the laboratory in ambient water, measured and
206 carefully dissected to collect their adductor muscle. The muscle tissues were then rinsed with
207 distilled water and preserved separately at -30°C until further analysis.

208

209 *In situ abundance of plankton in the Thau lagoon*

210 Phytoplankton, microzooplankton and mesozooplankton samples were collected at the pelagic
211 monitoring site, every two weeks from January to June 2017 and monthly onwards, until
212 December 2017. For phytoplankton, 10 to 20L of surface water were collected, filtered with a

213 15- μ m-mesh net, and preserved with 2% buffered formaldehyde. For microzooplankton, a
214 subsample of 30 ml of surface water was preserved with 2% buffered formaldehyde (to
215 estimate ciliates' abundance) and one of 110 ml was preserved with Lugol's solution (to
216 estimate heterotrophic flagellates' abundance). Phytoplankton and microzooplankton species
217 were identified and counted using sedimentation chambers and an inverted microscope
218 (Olympus IX70) following the Utermöhl method (Utermöhl 1958). Mesozooplankton samples
219 were collected near the surface by horizontal towing using a modified WP2 plankton net (1.2
220 m long, 50-cm opening, and 200- μ m mesh). Samples were immediately preserved in 4%
221 buffered formaldehyde until further analysis in the laboratory. Mesozooplankton abundance
222 was determined by counting organisms under a dissecting microscope (Olympus SZX7 –
223 ILLT). The diversity of mesozooplankton was not assessed.

224

225 *Gut content analyses*

226 To evaluate the diet of *A. coerulea* medusae, their gastric pouches, oral arms, and the
227 preserving solution were examined under a dissecting microscope (Olympus SZX7 – ILLT).
228 Although *A. coerulea* medusae were present in the lagoon from March, most individuals
229 exhibited empty guts during this month. Therefore, gut content analysis was only performed
230 on the medusae collected between April and June. For this, only complete exoskeletons were
231 considered for prey identification. This was done to the lowest possible taxonomic level,
232 although the level of exoskeleton digestion often precluded prey identification down to the
233 species level. The importance of each prey in the diet was expressed by the following indices:
234 (i) the frequency of occurrence (in %), which represents the percentage of medusae with the
235 prey *i* in their guts among all those that had non-empty guts; (ii) the index of relative
236 importance (in %), representing the percentage of prey *i* in relation to the total number of prey

237 items found in the non-empty guts; and (iii) the mean abundance of prey *i* in non-empty guts
238 (in ind. medusae⁻¹).

239

240 *Stable isotope analysis*

241 All filters containing plankton (phytoplankton, microzooplankton, and mesozooplankton)
242 were oven-dried at 60°C for 48h and the biological material was gently scraped off the filter
243 surface. Samples for the sedimentary organic matter, the oysters, *A. coerulea* medusae,
244 scyphistomae, and ephyrae were freeze-dried for 48h and ground to a fine powder using a
245 mortar and pestle. The sedimentary organic matter samples were divided into two subsamples.
246 One half was used directly for N stable isotope analysis. The remaining subsample was
247 acidified with 1% HCl to remove carbonates before C stable isotope analysis, rinsed several
248 times with distilled water, and oven-dried at 70°C.

249 Stable isotopic analyses for biological samples were performed using a PDZ Europa ANCA-
250 GSL elemental analyser interfaced with a PDZ Europa 20-20 isotope ratio mass spectrometer
251 (Sercon Ltd., Cheshire, UK). Measurements of $\delta^{13}\text{C}$ and $\delta^{15}\text{N}$ signatures were performed each
252 on 1.5 to 4 mg of dry samples, with exception of the medusae, for which ca. 10 mg of dry
253 sample was required for successful analysis, after salt content correction, based on dry weight
254 and ash-free dry weight relationships (Lucas et al. 1994; Pitt et al. 2009). Sedimentary organic
255 matter samples (of ca. 55 mg each) were analysed using an Elementar Vario EL Cube or
256 Micro Cube elemental analyser (Elementar Analysensysteme GmbH, Hanau, Germany)
257 interfaced to a PDZ Europa 20-20 isotope ratio mass spectrometer (Sercon Ltd., Cheshire,
258 UK). Calibration was performed against NIST Standard Reference Materials (IAEA-600,
259 USGS-40, USGS-41, USGS-42, USGS-43, USGS-61, USGS-64, and USGS-65). Isotope
260 ratios of all samples were expressed as parts per thousand (‰) differences from the internal

261 reference standards (glutamic acid, alfalfa flour, nylon 6, bovine liver, and enriched alanine)
262 using the following equation:

$$263 \quad \delta X = \left[\left(\frac{R_{sample}}{R_{standard}} \right) - 1 \right] \times 1000$$

264 where X is the ^{13}C or ^{15}N and R is the corresponding ratio, $^{13}\text{C}/^{12}\text{C}$ or $^{15}\text{N}/^{14}\text{N}$.

265 As the lipid content of organisms affects their $\delta^{13}\text{C}$ signatures, $\delta^{13}\text{C}$ correction is required

266 when C:N is higher than 3.5 (Post et al. 2007). Therefore, the $\delta^{13}\text{C}$ values obtained for *A.*

267 *coerulea* scyphistomae and medusae (mean C:N 3.7 ± 0.1 and 3.9 ± 0.6 , respectively) and for

268 the mesozooplankton (mean C:N of 6.9 ± 3.0) were corrected ($\delta^{13}\text{C}_{corr}$) according to the

269 equations proposed by D'Ambra et al. (2014) for jellyfish:

$$270 \quad \delta^{13}\text{C}_{corr} = \delta^{13}\text{C}_{initial} - 9.43 + 2.69 \times C:N$$

271 and by Syväranta and Rautio (2010) for zooplankton:

$$272 \quad \delta^{13}\text{C}_{corr} = \delta^{13}\text{C}_{initial} + 7.95 \times \left(\frac{C:N - 3.8}{C:N} \right)$$

273

274

275 *Relationship between benthic population dynamics and plankton abundance*

276 Data on *A. coerulea* benthic population dynamics were obtained from Marques et al. (2019).

277 Generalized linear models (using linear and logistic regressions, without interactions) were

278 employed to assess the respective contributions of the absolute abundances of the non-

279 averaged phytoplankton, the microzooplankton and the mesozooplankton (after logarithmic

280 transformation $\ln(x+1)$) to temporal trends in the scyphistomae density (% coverage) and in

281 the proportion of the scyphistomae producing buds. The models were validated by

282 examination of residuals versus fitted values plots (Zuur et al. 2009).

283

284 *Determination of Isotopic Niche Periods*

285 To reveal potential shifts in the trophic niches of *A. coerulea* scyphistomae and medusae
286 during the year and identify the periods when they present unchanging isotopic signatures
287 (hereafter "Isotopic Niche Periods"), a cluster analysis was performed on the monthly mean
288 isotopic values of both life stages (Jain 2010). For this, partitioning algorithms, based on the
289 k-means clustering method, were applied using the package "factoextra" (Kassambara and
290 Mundt 2017). The k-means approach subdivides the data into a set of k groups so that the sum
291 of squares from the data points to the center of each group is minimized (Kassambara and
292 Mundt 2017). This clustering approach allowed to identify the successive isotopic niche
293 periods for both life stages, providing the basis for identifying their successive sources of
294 organic matter during the year.

295

296 *Assessment of potential intra- and interspecific trophic competition*

297 Our sampling design allowed for reliable estimation of the potential intraspecific trophic
298 competition between *A. coerulea* scyphistomae and medusae within each isotopic niche
299 period. However, because oyster and jellyfish samples were collected in different years
300 (except for one isotopic niche period), the trophic competition between the two species was
301 only investigated globally, assuming that interannual variability in the trophic niche in the two
302 species is negligible. In both cases, the Bayesian framework proposed by Jackson et al. (2011)
303 for evaluating trophic competition was used. For this, Bayesian multivariate normal
304 distributions were first fitted to the isotopic signatures of all organisms. Then, the overlap
305 between their trophic niches was calculated based on maximum likelihood fitted ellipses,
306 using the function "maxLikOverlap" from the R package "SIBER" (Jackson et al. 2011).

307

308 *Determination of jellyfish diet using Stable isotope analysis*

309 Differences in isotopic signatures ($\delta^{13}\text{C}$ and $\delta^{15}\text{N}$) among the main local potential food
310 sources (phytoplankton, microzooplankton, mesozooplankton, and sedimentary organic
311 matter) were tested by a PERMANOVA (Anderson 2017) on the log10 transformed Bray-
312 Curtis distance matrix ($-\delta^{13}\text{C}$ and $\delta^{15}\text{N}$), made using the package “vegan” (Oksanen et al.
313 2019), followed by pairwise comparisons made using the “pairwiseAdonis” package in R
314 (Martinez Arbizu 2019). Sources with no significant differences were grouped for subsequent
315 analyses.

316 Diet compositions for *A. coerulea* scyphistomae and medusae within each isotopic niche
317 period were assessed using Bayesian mixing models developed specifically for stable isotope
318 analysis (“MixSIAR” package, Stock and Semmens 2016). By generating the probability
319 distributions of all potential mixing solutions with the associated confidence intervals (based
320 on 300 000 chain length), this approach allows identifying the most likely contribution for
321 each food source. MixSIAR further provides a graphical user interface that allows
322 investigation of the contributions of multiple food sources to the diet of target predators,
323 considering not only the isotopic signatures ($\delta^{13}\text{C}$ and $\delta^{15}\text{N}$) of the sources and the predators
324 but also the uncertainties and variability around these estimates. Finally, the method allows us
325 to use different isotopic fractionation factors at each trophic level. As previously performed in
326 other studies on jellyfish diet (e.g. Morais et al. 2017), the fractionation values applied here
327 for both *A. coerulea* life stages were those proposed by Vander Zanden and Rasmussen
328 (2001): for $\delta^{13}\text{C}$ we used 0.47 ± 1.23 ‰ in all cases, while for $\delta^{15}\text{N}$ we used 2.52 ± 2.5 ‰ and
329 3.23 ± 0.41 ‰ according to the type of food consumed (plant vs. animal, respectively). Like
330 Fleming et al. (2015) and Milisenda et al. (2018), we did not use the fractionation values
331 reported by D’Ambra et al. (2014), since they are very distinct from those mostly used in the
332 literature (Vander Zanden and Rasmussen 2001; Post 2002) and they still require further
333 laboratory corroboration (D’Ambra et al. 2014).

334 The basal tissue turnover rate for *Aurelia* sp. is of ca. 1 ‰ day⁻¹ for δ¹³C and 2‰ day⁻¹ for
335 δ¹⁵N, and it takes 18 to 20 days for the tissues of this jellyfish to reach the stable isotopic
336 equilibrium with the food ingested (D'Ambra et al. 2014). To account for such turnover rates,
337 MixSIAR models were run by isotopic niche period, but jellyfish signatures at a given
338 sampling date were matched with those recorded one month earlier for all potential food
339 sources.

340

341 **Results**

342 *Medusae gut contents*

343 Among the 25 medusae collected for gut content analysis from April to June 2017, 21 had
344 food in their guts. The bell diameter of these individuals did not vary significantly over time
345 (ANOVA, $F_2 = 1.4$, p -value = 0.2), remaining at ca. 8.5 cm. Overall, gut content composition
346 predominantly consisted of mesozooplankton (>88%). Microzooplankton (mainly tintinnids)
347 and phytoplankton (mainly diatoms and dinoflagellates) represented only 8 and 4% of the
348 total prey identified, respectively, and they were only found in the guts in April and May (Fig.
349 2, Table 1, Supplementary Table 1). In April, phytoplankton and microzooplankton occurred
350 in 20 and 60% of the guts analysed, but their relative importance and abundances were still
351 low (< 7.5% and < 2.2 ind.medusa⁻¹, respectively, Table 1). In May, frequency of occurrence
352 increased for phytoplankton (33%) and slightly decreased for microzooplankton (56%) and
353 showed a growing trend of their relative importance for both groups (5.6 and 12.5%,
354 respectively, Fig. 2). Indeed, in May, microzooplankton relative importance was higher than
355 some mesozooplankton organisms, like the “other crustaceans” group, which includes
356 cladocerans and ostracods (10.0%; Table 1, Supplementary Table 1). Masses of unidentified
357 organic matter were also recurrently observed over the entire study period.

358 Twenty-four different taxa of mesozooplankton were identified in the guts of the medusae,
359 but, among them, copepods and nauplii (from cirripeds and copepods) dominated. They
360 occurred in 40 to 88.9% of the guts analysed and represented up to 46.3% of the prey
361 identified (in June, Table 1). The maximum average abundance of mesozooplankton
362 organisms in the guts (26.2 ± 35.4 ind.medusae⁻¹) was recorded in April when non-crustacean
363 taxa (mainly gastropod veliger), and copepods represented more than 80% of the prey
364 identified in medusae gut contents (Table 1). Nauplii (index of relative importance = 31.3%)
365 were the most important mesozooplanktonic prey in the guts in May, while in June, copepods
366 dominated (index of relative importance = 46.3%, Table1).

367

368 *Prey availability and relationship with benthic population dynamics*

369 Prey abundances in *A. coerulea* medusae gut contents did not reflect their availability in the
370 water column. The abundances of phytoplankton, microzooplankton, and mesozooplankton in
371 the lagoon all showed high intra-annual variability (Fig. 3), with respective peaks in January
372 ($25\,138 \pm 34\,047$ cell.L⁻¹) and May ($35\,794 \pm 18\,374$ and cell.L⁻¹), in February, April, and
373 September ($> 6\,200$ cell.L⁻¹) and in June ($90\,895 \pm 107\,072$ ind.m⁻³). Thus, when *A. coerulea*
374 medusae were present in the water column, the planktonic community was mainly dominated
375 by phytoplankton in April and May, and by mesozooplankton in March and June, while the
376 microzooplankton showed consistently lower abundances despite a small peak in April. In
377 terms of species composition, the most abundant phytoplanktonic and microzooplanktonic
378 taxa in the water column during the study period were *Chaetoceros* sp. and *Strombidium* sp.,
379 respectively (Supplementary Table 2). Mesozooplankton diversity was not assessed, but
380 *Acartia* sp. are recurrently the most abundant taxa in Thau (Boyer et al. 2013).
381 Annual variations in scyphistomae coverage, which peaked in April (11.6 ± 3.7 %, Marques
382 et al. 2019), were positively correlated with the non-averaged abundance of phytoplankton

383 (Generalized linear models, t-value = 2.97, p-value = 0.01, Table 2, Fig. 4). In turn,
384 fluctuations in the mean percentage of scyphistomae producing buds, which varied between
385 0.4 ± 0.7 % in November and 25.2 ± 7.3 % in September (Marques et al. 2019, Fig. 4), were
386 positively correlated with variations in non-averaged microzooplankton abundance
387 (Generalized linear models, t-value = 10.19, p-value < 0.01, Table 2).

388

389 *Temporal variation of A. coerulea isotopic signatures*

390 $\delta^{13}\text{C}$ and $\delta^{15}\text{N}$ signatures showed significant temporal variation for both the scyphistomae and
391 medusae (one-way PERMANOVA, Pseudo- $F_{11} = 22.7$, p-value < 0.01 and Pseudo- $F_3 = 38.6$,
392 p-value = 0.001, respectively), but differences between life stages were never significant
393 during the period of medusae presence, from March to June (one-way PERMANOVA,
394 Pseudo- $F_1 = 1$, p-value = 0.4). The mean bell diameter of the medusae used for stable isotope
395 analysis, showed a sharp increase between March (1.0 ± 0.3 cm) and June (8.9 ± 1.1 cm), with
396 an estimated overall growth of $0.8 \text{ mm}\cdot\text{day}^{-1}$. Over this period, medusae $\delta^{13}\text{C}$ signatures
397 increased progressively from $-23.4 \pm 0.1\text{‰}$ to $-19.4 \pm 0.5\text{‰}$, while their $\delta^{15}\text{N}$ signatures
398 remained stable for the first three months (at ca. 8.1‰), and increased (to a maximum at $8.9 \pm$
399 0.3‰) only in June (Fig. 5). For the scyphistomae, minimum $\delta^{13}\text{C}$ values were registered at
400 the beginning of the study period (in January 2017, mean: $-23.4 \pm 0.1\text{‰}$). The $\delta^{13}\text{C}$ signatures
401 then increased to reach maximum values in June, July, and August ($> -19.4\text{‰}$) before
402 decreasing again until January 2018 ($-22.3 \pm 0.4\text{‰}$). The $\delta^{15}\text{N}$ signatures of scyphistomae
403 showed a similar temporal trend, with low values at the beginning and the end of the study
404 period ($8.3 \pm 0.1\text{‰}$ and $8.0 \pm 0.4\text{‰}$ in January 2017 and 2018, respectively), and maximum
405 values in July and August ($>9\text{‰}$). The minimum values of $\delta^{15}\text{N}$ signatures, though, were
406 observed in February 2017 ($7.1 \pm 0.5\text{‰}$). The average $\delta^{13}\text{C}$ and $\delta^{15}\text{N}$ signatures of the ephyrae
407 collected in January 2018 (bell diameter of 0.21 ± 0.1 cm) were of $-22.8 \pm 0.1\text{‰}$ and $8.5 \pm$

408 0.3‰, respectively. They did not differ significantly from those of the scyphistomae collected
409 at the same sampling time (T-test, $t = -1.9$, $df = 2.3$ p-value = 0.2 and $t = 1.2$, $df = 2.6$, p-value
410 = 0.3, for $\delta^{13}\text{C}$ and $\delta^{15}\text{N}$ respectively).

411 The clustering analysis revealed three distinct groups of isotopic signatures among the
412 monthly values obtained for all life stages of *A. coerulea* (Fig. 6) allowing to identify three
413 isotopic niche periods during the year.: Period 1 gathered the $\delta^{13}\text{C}$ and $\delta^{15}\text{N}$ signatures of all
414 life stages from December to April, irrespective of the year (2017 or 2018). Period 2 reflected
415 the signatures of both the medusae and the scyphistomae from June to August. Period 3
416 corresponded to the signatures of the scyphistomae from September to November, together
417 with the signatures of the medusae and the scyphistomae in May. However, May showed a
418 particular sharp shift in $\delta^{13}\text{C}$ and $\delta^{15}\text{N}$ reflecting the rapid transition from the isotopic
419 signature of period 1 to that of period 2 and, therefore, it was not included in any isotopic
420 niche period.

421

422 *Monthly variability of organic matter sources signatures*

423 $\delta^{13}\text{C}$ and $\delta^{15}\text{N}$ signatures varied significantly according to the organic matter source and the
424 month (significant interaction, PERMANOVA, $Pseudo-F_{17} = 23.1$, p-value < 0.01; Fig. 7).
425 For carbon signatures, minimum $\delta^{13}\text{C}$ values for phytoplankton, microzooplankton and
426 mesozooplankton (of -24.7 ± 0.3 , -23.3 ± 0.1 and -23.7 ± 0.0 ‰, respectively) were all
427 observed in March. A sharp increase in $\delta^{13}\text{C}$ was observed in the following months, with
428 maximums in May for mesozooplankton (-18.8 ± 0.2 ‰) and in November for phytoplankton
429 (-19.0 ± 0.0 ‰) and microzooplankton (19.9 ± 0.1 ‰). Concerning nitrogen signatures,
430 mesozooplankton was the organic matter source with the highest $\delta^{15}\text{N}$ values, ranging from
431 7.3 ± 0.3 (in May) to 8.4 ± 0.0 ‰ (in March). Minimum $\delta^{15}\text{N}$ values were also observed in
432 May for the phytoplankton and the microzooplankton (at 5.8 ± 0.5 ‰ and 6.0 ± 0.3 ‰,

433 respectively) but, for these two organic matter sources, maximum values were observed in
434 July (at 6.7 ± 0.3 ‰ and 7.4 ± 0.2 ‰, respectively). Moreover, another peak in $\delta^{15}\text{N}$ (at $6.7 \pm$
435 0.0 ‰) was observed in February for the phytoplankton. For the sedimentary organic matter,
436 both the $\delta^{13}\text{C}$ and $\delta^{15}\text{N}$ signatures decreased from March (-18.9 ‰ and 5.8 ‰, respectively) to
437 April (-20.7 ‰ and 5.5 ‰, respectively), remaining constant afterwards.

438

439 *Contribution of organic matter sources to A. coerulea isotopic signatures*

440 Since the $\delta^{13}\text{C}$ and $\delta^{15}\text{N}$ signatures of the phytoplankton and the microzooplankton were not
441 significantly different (PERMANOVA post-hoc test, Pseudo- $F_1 = 5.7$, adjusted p-value =
442 0.17) these two organic matter sources were pooled as Small Plankton group in the mixing
443 models used to assess the diet of *A. coerulea*. The remaining sources were included
444 individually in the models (Table 3). The contribution of each source was found to vary
445 according to the isotopic niche periods and the life stage of *A. coerulea* considered (Fig. 8).
446 For the scyphistomae, the model suggested a dietary shift from small plankton consumption in
447 period 1 (93.3%) to a diet based on a mix of benthic (36.6% of sedimentary organic matter)
448 and pelagic (39.3% of mesozooplankton and 24.4% of small plankton) sources in period 2.
449 The same occurred in period 3, although the small plankton was the main food source
450 (69.2%), and sedimentary organic matter contribution decreased (27.0%). For the medusae,
451 small plankton was the only food source (100%) in period 1, but the diet changed in period 2,
452 including mainly sedimentary organic matter (64.3%) and mesozooplankton (32.3%). As the
453 isotopic signatures of the ephyrae collected in January 2018 were very similar to those of the
454 scyphistomae in the same period, their diet probably mainly consist of small plankton
455 organisms.

456

457 *Intra- and interspecific competitions for the food resources*

458 Intraspecific isotopic niche overlap was substantial during the whole period of co-occurrence
459 of the benthic and pelagic stages of *A. coerulea* in the lagoon (March to June; Fig. 9). Indeed,
460 although the percentage of niche overlap was higher in period 1 (41.5%) than in period 2
461 (only 9.9%), the isotopic niche of the medusae entirely overlaid that of the scyphistomae in
462 period 2. Similarly, although only three ephyrae samples were analysed in this study (all from
463 January 2018), their isotopic signatures were close to those observed for the scyphistomae in
464 period 1, suggesting high (although not quantifiable) trophic niche overlap among these two
465 life stages.

466 In Thau, interspecific trophic competition between *A. coerulea* and bivalves was observed,
467 although limited. The $\delta^{13}\text{C}$ and $\delta^{15}\text{N}$ signatures of the oysters from the lagoon varied from –
468 25.6 to -18.5‰ and from 8.4 to 9.4‰, respectively (Fig. 10). Significant differences in
469 isotopic signatures were observed between cultivated and wild individuals (PERMANOVA,
470 Pseudo- $F_{11} = 12.4$, p-value < 0.01 ; Fig. 10), with the former showing significantly higher $\delta^{13}\text{C}$
471 ($-19.7 \pm 0.9\text{‰}$) and lower $\delta^{15}\text{N}$ ($8.6 \pm 0.3\text{‰}$) signatures on average than the later ($-20.1 \pm$
472 0.4‰ and $9.2 \pm 0.3\text{‰}$, respectively). Interspecific isotopic niche overlaps were limited
473 ($<30\%$) and lower than that between cultivated and wild oysters (35.4%). Interspecific
474 isotopic niche overlap was more important between cultivated oysters and *A. coerulea* medusa
475 stage (29.1%). However, if we assume that the seasonal shifts in isotopic signatures are
476 consistent among years for both the jellyfish and the oysters, the trophic competition for food
477 should only occur at a limited period of the year and only with the medusae stage. Indeed,
478 only the signatures recorded in period 2 were responsible for the interspecific niche overlap
479 observed among *A. coerulea* medusae and cultivated (21.8%) or wild (21.1%) oysters.

480

481 **Discussion**

482 To our knowledge, this is the first study to investigate the trophic ecology of both the benthic
483 and the pelagic stages of a jellyfish species (*A. coerulea*) in association with its in situ
484 population dynamics and the plankton availability. The results obtained offer the
485 unprecedented opportunity to identify the bottom-up processes regulating *A. coerulea*
486 populations, contributing to our understanding of the formation of its blooms.

487

488 *Trophic ecology of the pelagic stages of A. coerulea*

489 Ephyrae were only collected once during the study period and their isotopic signature was
490 similar to that of scyphistomae at the same time, indicating major importance of the small
491 planktonic organic matter (i.e. phytoplankton and microzooplankton) in their diet. This result
492 will have to be confirmed because, in Thau, *A. coerulea* ephyrae are mainly released in
493 November, but strobilation continues until April (Marques et al. 2019). Therefore, we cannot
494 exclude that the ephyrae caught in January 2018 had been released just a few days or weeks
495 before their collection and therefore still had the isotopic signature of the scyphistomae that
496 produced them. Moreover, because of their very low growth rate during the winter (< 0.1
497 $\text{mm}\cdot\text{day}^{-1}$, Marques et al. 2015b), the ephyrae caught in January might not have yet
498 incorporated the signature of the prey ingested after their release (Frazer et al. 1997).
499 Nevertheless, phytoplankton, microzooplankton (such as rotifers) and suspended particulate
500 organic matter have all been previously identified as important food sources for ephyrae
501 (Båmstedt et al. 2001; Zheng et al. 2015) so our findings are in agreement with the literature.
502 The results from medusae gut contents analysis support previous reports describing *A.*
503 *coerulea* medusae as mesozooplanktivorous, feeding mainly on copepods and nauplii (mainly
504 of cirripeds). Indeed, *Aurelia* spp. medusae have been suggested to prey mainly on
505 mesozooplankton and to have higher clearance rates and selective preferences for crustacean
506 prey such as copepods, cirriped nauplii, and cladocerans (Hansson 2006; Lo and Chen 2008).

507 Phytoplankton and microzooplankton also contributed to the diet of *A. coerulea* medusae in
508 Thau, but only during their first two months of growth and with low relative importance.
509 Indeed, *Aurelia* spp. diet often echoes prey local abundances in their environment (e.g. Ishii
510 and Tanaka 2001), which might explain these results, since the abundance of
511 microzooplankton and phytoplankton in the lagoon were higher in April and May. Yet,
512 variations of prey availability in Thau were not entirely reflected in *A. coerulea* medusae diet,
513 since mesozooplankton represented consistently more than 80% of the prey identified in their
514 guts, despite its lower in situ abundance in this period. Although gut content analyses
515 provided important qualitative information on the diet of jellyfish medusae, conclusions
516 regarding the importance of each prey type for their growth, at longer time scales, should be
517 drawn with caution, due to the bias associated with this technique. The digestion time of
518 mesozooplankton in the medusae guts might vary between 1 and 5h, depending on medusa
519 size, temperature, and prey type (Ishii and Tanaka 2001; Martinussen and Båmstedt 2001),
520 with smaller prey being digested faster (Martinussen and Båmstedt 2001). Therefore, gut
521 content analysis often leads to an overestimation of the importance of hard and big prey in the
522 diet, such as crustaceans. This might have contributed to a general overlook of the potential
523 relevance of the lower trophic levels to the diet of jellyfish (Javidpour et al. 2016). Indeed, in
524 Thau, the diet composition of *A. coerulea* medusae differed between gut content and stable
525 isotope analyses. The later approach underlined not only the importance of the phytoplankton
526 and microzooplankton (pooled as small plankton) for the diet of *A. coerulea* medusae in Thau
527 but also that of the sedimentary organic matter.

528 The diet of the *A. coerulea* medusae varied over time. In general, the $\delta^{13}\text{C}$ (–23.4 to –19.4‰)
529 and $\delta^{15}\text{N}$ (8.1 to 8.9‰) values found for the *A. coerulea* medusae stage were in the range of
530 the values published by Fleming et al. (2015) (–20.3 to –18.1 for $\delta^{13}\text{C}$ and 8.5 to 11.8 for
531 $\delta^{15}\text{N}$) and D’Ambra et al. (2013) ($-20.5 \pm 0.3\text{‰}$ and $7.2 \pm 0.4\text{‰}$ on average for $\delta^{13}\text{C}$ and

532 $\delta^{15}\text{N}$, respectively). However, intra-annual fluctuations in medusae isotopic signatures
533 revealed a significant shift in May, with an increase of ca. 3.5 and 1‰ for $\delta^{13}\text{C}$ and $\delta^{15}\text{N}$,
534 respectively. This separates two distinct periods of stable isotopic signatures: period 1, during
535 medusae growth from March to April, and period 2, in June, when they reproduce before the
536 collapse of the bloom. This variation in the isotopic signature might indicate a rapid ontogenic
537 shift in the diet of the medusae, reflecting the change from small plankton to
538 mesozooplankton and sedimentary organic matter sources. A similar shift in the trophic niche
539 was also shown for *Aurelia aurita* in Northern Ireland, where medusae fed on higher trophic
540 levels by the end of their growing period (Fleming et al. 2015). Temporal variations in
541 isotopic signatures of predators might also reflect analogous changes in the isotopic signatures
542 at the base of the food webs (Post 2002). In this study, the values of the assessed organic
543 matter sources agree with those previously reported in Thau (Pernet et al. 2012) and other
544 north-western Mediterranean coastal lagoons (Dierking et al. 2012; Escalas et al. 2015) but
545 revealed significant fluctuations over time. In Thau, ^{13}C -depleted coastal inputs are dependent
546 on the rainfall, which was high in March and low in April ([http://www.meteofrance.fr/climat-](http://www.meteofrance.fr/climat-passe-et-futur/bilans-climatiques/bilan-2017)
547 [passe-et-futur/bilans-climatiques/bilan-2017](http://www.meteofrance.fr/climat-passe-et-futur/bilans-climatiques/bilan-2017). Accessed 27 Jul 2019), likely contributing to the
548 variation in the $\delta^{13}\text{C}$ isotopic signatures of the lower trophic levels and then reflected in those
549 of *A. coerulea* medusae. However, similar trends were not observed for $\delta^{15}\text{N}$ isotopic
550 signatures, which showed a decreasing trend for most organic matter sources in May,
551 contrasting with an increasing trend for medusae in June. This underlines that the observed
552 isotopic niche shift for *A. coerulea* medusae was not only a reflection of temporal fluctuations
553 in the signatures of their prey but likely induced by a significant change in their diet. Finally,
554 our results highlight the importance of sedimentary organic matter (64.3%) in the diet of *A.*
555 *coerulea* medusae, as previously observed for *A. aurita* in the Kiel Fjord (Javidpour et al.
556 2016). Like most shallow marine ecosystems, the Thau lagoon is recurrently subjected to

557 sediment resuspension, triggered by river floods and strong wind activity (Fouilland et al.
558 2012). With this regard, the unidentified masses of organic matter found in the guts of the
559 medusae were probably aggregates of re-suspended sedimentary organic matter.

560

561 *Trophic ecology of the benthic stage of A. coerulea*

562 The temporal variability of the $\delta^{13}\text{C}$ and $\delta^{15}\text{N}$ signatures of *A. coerulea* scyphistomae
563 suggested two significant intra-annual shifts in their diet and identified three different isotopic
564 niche periods. The diet of scyphistomae was mostly based on small plankton during period 1,
565 included all available food sources during period 2 and changed to a mix of pelagic (i.e., small
566 plankton) and sedimentary organic matter during period 3. These seasonal variations agree
567 with those of the availability of planktonic food sources in the lagoon, following the high
568 abundances of phytoplankton and microzooplankton in periods 1 and 3 and that of
569 mesozooplankton in period 2 (i.e., in June). Our results agree with the few existing reports on
570 the diet of jellyfish scyphistomae, which suggested that they feed on small mesozooplankton
571 species (e.g. copepods, cladocerans, and cirripeds nauplii; Östman 1997; Ikeda et al. 2017), as
572 well as on microzooplankton and phytoplankton (dinoflagellates, ciliates, rotifers, and
573 diatoms; Kamiyama 2013; Wang et al. 2015; Huang et al. 2015). However, as for medusae,
574 the temporal variation in scyphistomae isotopic signatures might also reflect the origin of the
575 carbon and nitrogen inputs in the lagoon (Post 2002). Indeed, fluctuations in $\delta^{13}\text{C}$ and $\delta^{15}\text{N}$
576 values might reflect the stronger contribution of terrestrial inputs to the basis of the food web,
577 after rainy events in period 1 (Vizzini et al. 2005; Pernet et al. 2012a) and the exceptionally
578 low terrestrial inputs from June onwards (periods 2 and 3), due to a very dry summer and
579 autumn in 2017 (> 80% loss of rainfall when compared with the mean between 1981 – 2010
580 in October, <http://www.meteofrance.fr/climat-passe-et-futur/bilans-climatiques/bilan-2017>.
581 Accessed 27 Jul 2019). Furthermore, it might also be affected by the higher influence of

582 wastewater effluent in the lagoon during dry periods (Perrin and Tournoud 2009), which is
583 suggested to induce an enrichment of $\delta^{15}\text{N}$ signatures, as in other coastal lagoons (Vizzini et
584 al. 2005; Dierking et al. 2012; Escalas et al. 2015). Yet, the skewed temporal pattern of the
585 scyphistomae isotopic signatures when compared with their sources further confirm a
586 seasonal variation in their diet.

587 The increase in mesozooplankton consumption during period 2, when the abundance of this
588 prey is maximal, is not surprising. Higher abundances of this type of prey (especially of newly
589 hatched *Artemia* sp.) is recognized to induce better performances of scyphistomae (i.e.,
590 growth, asexual reproduction, and strobilation) in laboratory experiments (e.g. Ikeda et al.
591 2017; Hubot et al. 2017). However, our results further highlight the prominent role of the
592 lower trophic levels in the feeding and benthic population dynamics of the species in Thau.

593 Although we were not able to precisely quantify the relative importance of phytoplankton and
594 microzooplankton in the diet of *A. coerulea* scyphistomae, they both appear to be important.
595 Phytoplankton cells are seemingly insufficient to support scyphistomae basic metabolic rates
596 at high temperatures (20°C) and for long periods (Wang et al. 2015; Huang et al. 2015), but
597 they provide a suitable alternative source of energy for their survival and asexual reproduction
598 at low temperatures (Huang et al. 2015; Wang et al. 2015). Therefore, peaks in phytoplankton
599 abundances during period 1 probably support *A. coerulea* scyphistomae survival over the
600 winter and early spring. Similarly, the significant positive correlation between the abundance
601 of microzooplankton and the percentage of scyphistomae producing buds suggests that this
602 type of prey promotes the buds production, ultimately driving the benthic population density.

603 Indeed, buds production by scyphistomae of *Aurelia aurita* has been previously shown to
604 increase when reared on a ciliate-based diet rather than on the larger *Artemia* prey (Kamiyama
605 2013). Interestingly, although more buds were produced in April in the lagoon (due to high
606 scyphistomae density) the peak of the percentage of scyphistomae producing buds, as well as

607 the maximum number of buds per scyphistoma, were registered in September (Marques et al.
608 2019), co-occurring with high abundances of microzooplankton in the lagoon.
609 Lastly, as for medusae, our results highlight the importance of the sedimentary organic matter
610 in the diet of *A. coerulea* scyphistomae in Thau. This does not come as a major surprise
611 because re-suspended sediments were often observed on the scyphistomae samples collected
612 *in situ*. Sedimentary organic matter is usually composed by a mixture of microphytobenthos,
613 heterotrophic microorganisms (bacteria, ciliates, protozoans, nematodes) and detritus,
614 classically associated and re-suspended with sediment (Dubois et al. 2007), which might
615 provide a suitable source of food for jellyfish benthic stages (Östman 1997).

616

617 *Intra- and interspecific competition*

618 The benthic scyphistomae and the pelagic medusae of *A. coerulea*, although inhabiting
619 different habitats, appeared to share, at least partially, the same organic matter sources in the
620 lagoon. During period 1, their high isotopic niche overlap, and the results of the mixing
621 models, indicate that both stages feed on phytoplankton and/or microzooplankton. In period 2,
622 despite a lower isotopic niche overlap, the trophic niche of the medusae entirely covers that of
623 the scyphistomae. This suggests that during large medusae blooms and under food limitation
624 conditions, intraspecific competition for food might occur in the lagoon, with possible
625 detrimental impacts on the scyphistomae population.

626 One of the main concerns regarding the presence of *A. coerulea* in Thau is the potential
627 competition for food with the oysters produced in the lagoon, in particular during the medusae
628 blooms and due to the overspread distribution of scyphistomae (Marques et al. 2015a).

629 However, our results suggest only a limited trophic niche overlap. Although oysters and *A.*
630 *coerulea* stages were not collected in the same year (except in period 3) we assumed that the
631 isotopic signature of the oysters mostly varies intra-annually (Pernet et al. 2012). If this is

632 true, our results indicate that interspecific competition for food only potentially occurs
633 between *A. coerulea* medusae and oysters (cultivated and wild) in period 2. During this
634 period, sedimentary organic matter was an important source in the diet of *A. coerulea*
635 medusae and also reported as part of the diet of oysters (Dubois and Colombo 2014). This
636 might explain the isotopic niche overlap, although restricted, between these two organisms at
637 this period. The limited interspecific trophic competition between the *A. coerulea* and the
638 oysters might result from their different filtration and particle retention mechanisms, as
639 previously suggested for other suspension-feeding species co-occurring with oysters (Dubois
640 and Colombo 2014). Indeed, *A. coerulea* medusae are cruising predators, capturing their prey
641 using locally generated flow currents (Dabiri et al. 2005) and the scyphistomae use a passive
642 ambush strategy (Huang et al. 2015), contrasting with the true filter-feeding strategy of the
643 oysters (Dubois et al. 2007; Dubois and Colombo 2014). The different mechanisms to capture
644 prey, likely promoted the selection and ingestion of different organic matter sources, reducing
645 the trophic competition for the same type of prey. Phytoplankton (especially diatoms) is the
646 main source of food for oysters (Dupuy et al. 2000; Pernet et al. 2012). In situ feeding
647 experiments showed that the consumption of *Aurelia* sp. medusae on micro- and
648 mesozooplankton organisms released the predation pressure from these secondary producers
649 on the lower trophic levels, boosting phytoplankton biomass and bacterial production (Turk et
650 al. 2008). Therefore, it is possible that the blooms of *A. coerulea* medusae might even be
651 advantageous for the production of oysters in the lagoon, via a top-down cascade effect on the
652 microbial community.

653

654 *Bottom-up control of the A. coerulea population dynamics*

655 In the Thau lagoon, the winter and early spring are critical periods for the formation of
656 the *A. coerulea* bloom (Marques et al. 2019). The production of ephyrae occurs between

657 November and April, with two main peaks: in November (during period 3) due to a high
658 percentage of the scyphistomae strobilating (despite their low densities), and in February –
659 March (during period 1), when this percentage is low but the density of scyphistomae is high
660 (Marques et al. 2019). As they grow to become medusae, the magnitude of the bloom is thus,
661 tightly dependent on the accumulated production of ephyrae, their survival, and growth rate.
662 In period 1, phytoplankton and microzooplankton are the main sources of food for both the
663 ephyrae and scyphistomae of *A. coerulea*. This stresses the role of the lower trophic levels in
664 the formation of the local jellyfish blooms: they promote higher levels of scyphistomae and
665 ephyrae survival and they boost the production of buds, leading to higher scyphistomae
666 densities and ephyrae production. In summer (during period 2) both *A. coerulea* life stages
667 change their diet to a mix of all sources (except small plankton for medusae). This is
668 particularly important because it supports the peak of the bloom, following high growth rates
669 of medusae, as well as their sexual reproduction (Fig. 11; Marques et al. 2015b). It is also
670 during this period that scyphistomae coverage declines (Fig. 11, Marques et al. 2019). Our
671 results suggest a potentially high intraspecific trophic competition between scyphistomae and
672 medusae, especially during this period. Therefore, the high abundance and high predation
673 pressure of the medusae might lead to the reduction of food availability for scyphistomae and
674 could contribute to the reduction of their coverage. During the following dry season (i.e.,
675 period 3), a bacteria-based food web prevails in the lagoon, with internal regeneration of
676 nitrogen, due to the absence of terrestrial freshwater inputs in the lagoon (Chapelle et al.
677 2000). This likely supports the peaks of microzooplankton abundance since these organisms
678 are recognized as important bacterivorous (Rassoulzadegan and Sheldon 1986).
679 Microzooplankton appear to have a critical role as a source of food for scyphistomae, which,
680 in period 3, would sustain not only the noticed peak of buds production in September but also

681 the main strobilation period in November (Marques et al. 2019), i.e., the first peak of ephyrae
682 production and the initial foundation of the subsequent jellyfish bloom in the Thau lagoon.

683

684 *Limitation of the study*

685 Although stable isotope analysis is a powerful tool to assess the trophic ecology of predators,
686 the MixSIAR results should be considered with caution. Indeed, mixing models always
687 provide a solution but their results might not always be biologically relevant: their precision
688 decreases with the number of introduced organic matter sources and depends greatly on the
689 accuracy of their signatures (Dubois et al. 2007).

690 In this work, we used a turnover time of one month for both jellyfish life stages, following the
691 results reported for *Aurelia* sp. (18 – 20 days, D’Ambra et al. 2014). If inaccurate, this might
692 have significantly biased the MixSIAR results for each isotopic niche period because the set
693 of organic matter source signatures matching with those of the jellyfish might be incorrect.
694 Moreover, despite the frequency of sampling for organic matter sources during our study,
695 some periods of the year (e.g. July – September) were less represented in the database. Given
696 the intra-annual variability in the isotopic signatures of the plankton component, we cannot
697 fully exclude that this sampling gap slightly biased our results.

698 The implementation of different isotopic fractionation values in the mixing models also
699 drastically modify their final results. In our study, using the fractionation values proposed by
700 D’Ambra et al. (2014) would result in a higher contribution of mesozooplankton to the diet in
701 both stages of *A. coerulea*. However, the values from D’Ambra et al. (2014) are very different
702 from those typically reported in the literature (e.g. Vander Zanden and Rasmussen 2001; Post
703 2002), leading to unrealistic trophic levels (Fleming et al. 2015; Milisenda et al. 2018).
704 Furthermore, the temperature (which is highly variable in Thau), the feeding condition, the

705 sexual maturity (e.g. Barnes et al. 2007), and, probably, the life stage might also affect
706 fractionation and turnover values.

707

708 **Conclusion**

709 Knowledge of the trophic ecology and population dynamics of jellyfish is imperative
710 to understand the main environmental drivers of blooms. With this regard, the Thau lagoon
711 offered an exceptional framework to study both benthic and pelagic trophic interactions and to
712 uncover the main organic matter sources supporting key periods of the *A. coerulea* life cycle.
713 In particular, we highlight the role of phytoplankton and microzooplankton in supporting
714 scyphistomae survival and asexual reproduction, that of mesozooplankton and sedimentary
715 organic matter for the growth of medusae, as well as the possible negative influence of
716 intraspecific competition on the benthic population dynamics. Moreover, we demonstrate that
717 the interspecific trophic competition between *A. coerulea* and the commonly cultivated oyster
718 *C. gigas* is likely to be limited, at least in the Thau lagoon, and therefore, we advocate that *A.*
719 *coerulea* blooms have a seemingly restricted impact on the local shellfish production.

720

721

722

723

724

725

726

727 **References:**

- 728 Anderson MJ (2017) Permutational Multivariate Analysis of Variance (PERMANOVA). In:
729 Wiley StatsRef: Statistics Reference Online. John Wiley & Sons, Ltd, Chichester, UK,
730 pp 1–15. doi: 10.1002/9781118445112.stat07841
- 731 Båmstedt U, Wild B, Martinussen MB (2001) Significance of food type for growth of ephyrae
732 *Aurelia aurita* (Scyphozoa). Mar Biol 139:641–650. doi: 10.1007/s002270100623
- 733 Barnes C, Sweeting CJ, Jennings S, Barry JT, Polunin NVC (2007) Effect of temperature and
734 ration size on carbon and nitrogen stable isotope trophic fractionation. Funct Ecol
735 21:356–362. doi: 10.1111/j.1365-2435.2006.01224.x
- 736 Boero F, Bouillon J, Gravili C, Miglietta MP, Parsons T, Piraino S (2008) Gelatinous
737 plankton: irregularities rule the world (sometimes). Mar Ecol Prog Ser 356:299–310. doi:
738 10.3354/meps07368
- 739 Bonnet D, Molinero J-C, Schohn T, Daly-Yahia MN (2012) Seasonal changes in the
740 population dynamics of *Aurelia aurita* in Thau lagoon. Cah Biol Mar 53:343–347.
- 741 Boyer S, Bouvy M, Bonnet D (2013) What triggers *Acartia* species egg production in a
742 Mediterranean lagoon? Estuar Coast Shelf Sci 117:125–135. doi:
743 10.1016/j.ecss.2012.11.006
- 744 Chapelle A, Ménesguen A, Deslous-Paoli J-M, Souchu P, Mazouni N, Vaquer A, Millet B
745 (2000) Modelling nitrogen, primary production and oxygen in a Mediterranean lagoon.
746 Impact of oysters farming and inputs from the watershed. Ecol Modell 127:161–181. doi:
747 10.1016/S0304-3800(99)00206-9
- 748 Condon RH, Graham WM, Duarte CM, Pitt KA, Lucas CH, Haddock SHD, Sutherland KR,
749 Robinson KL, Dawson MN, Decker MB, Mills CE, Purcell JE, Malej A, Mianzan H,
750 Uye S-I, Gelcich S, Madin LP (2012) Questioning the Rise of Gelatinous Zooplankton in
751 the World’s Oceans. Bioscience 62:160–169. doi: 10.1525/bio.2012.62.2.9

752 D'Ambra I, Graham WM, Carmichael RH, Malej A, Onofri V (2013) Predation patterns and
753 prey quality of medusae in a semi-enclosed marine lake: implications for food web
754 energy transfer in coastal marine ecosystems. J Plankton Res 35:1305–1312. doi:
755 10.1093/plankt/fbt065

756 D'Ambra I, Carmichael RH, Graham WM (2014) Determination of $\delta^{13}\text{C}$ and $\delta^{15}\text{N}$ and trophic
757 fractionation in jellyfish: Implications for food web ecology. Mar Biol 161:473–480. doi:
758 10.1007/s00227-013-2345-y

759 Dabiri JO, Colin SP, Costello JH, Gharib M (2005) Flow patterns generated by oblate
760 medusan jellyfish: field measurements and laboratory analyses. J Exp Biol 208:1257 LP
761 – 1265. doi: 10.1242/jeb.01519

762 Dawson MN, Martin DL (2001) Geographic variation and ecological adaptation in *Aurelia*
763 *aurita* (Scyphozoa, Semaestomeae): some implications from molecular phylogenetics.
764 Hydrobiologia 451:259–273. doi: <https://doi.org/10.1023/A:1011869215330>

765 Dierking J, Morat F, Letourneur Y, Harmelin-Vivien M (2012) Fingerprints of lagoonal life:
766 Migration of the marine flatfish *Solea solea* assessed by stable isotopes and otolith
767 microchemistry. Estuar Coast Shelf Sci 104–105:23–32. doi: 10.1016/j.ecss.2011.03.018

768 Dubois S, Orvain F, Marin-Léal JC, Ropert M, Lefebvre S (2007) Small-scale spatial
769 variability of food partitioning between cultivated oysters and associated suspension-
770 feeding species, as revealed by stable isotopes. Mar Ecol Prog Ser 336:151–160. doi:
771 10.3354/meps336151

772 Dubois SF, Colombo F (2014) How picky can you be? Temporal variations in trophic niches
773 of co-occurring suspension-feeding species. Food Webs 1:1–9. doi:
774 10.1016/j.fooweb.2014.07.001

775 Dupuy C, Vaquer A, Lam-Höai T, Rougier C, Mazouni N, Lautier J, Collos Y, Le Gall S
776 (2000) Feeding rate of the oyster *Crassostrea gigas* in a natural planktonic community of

777 the Mediterranean Thau Lagoon. *Mar Ecol Prog Ser* 205:171–184. doi:
778 10.3354/meps205171

779 Escalas A, Ferraton F, Paillon C, Vidy G, Carcaillet F, Salen-Picard C, Le Loc’h F, Richard
780 P, Darnaude AM (2015) Spatial variations in dietary organic matter sources modulate the
781 size and condition of fish juveniles in temperate lagoon nursery sites. *Estuar Coast Shelf*
782 *Sci* 152:78–90. doi: 10.1016/j.ecss.2014.11.021

783 Fleming NEC, Harrod C, Newton J, Houghton JDR (2015) Not all jellyfish are equal: isotopic
784 evidence for inter- and intraspecific variation in jellyfish trophic ecology. *PeerJ* 3:e1110.
785 doi: 10.7717/peerj.1110

786 Fouilland E, Trottet A, Bancon-Montigny C, Bouvy M, Le Floc’h E, Gonzalez J-L, Hatey E,
787 Mas S, Mostajir B, Nougier J, Pecqueur D, Rochelle-Newall E, Rodier C, Roques C,
788 Salles C, Tournoud M-G, Vidussi F (2012) Impact of a river flash flood on microbial
789 carbon and nitrogen production in a Mediterranean Lagoon (Thau Lagoon, France).
790 *Estuar Coast Shelf Sci* 113:192–204. doi: 10.1016/j.ecss.2012.08.004

791 Frazer TK, Ross RM, Quetin LB, Montoya JP (1997) Turnover of carbon and nitrogen during
792 growth of larval krill, *Euphausia superba* Dana: a stable isotope approach. *J Exp Mar*
793 *Bio Ecol* 212:259–275. doi: 10.1016/S0022-0981(96)02740-2

794 Han C-H, Uye S-I (2010) Combined effects of food supply and temperature on asexual
795 reproduction and somatic growth of polyps of the common jellyfish *Aurelia aurita* s.l.
796 *Plankt Benthos Res* 5:98–105. doi: 10.3800/pbr.5.98

797 Hansson LJ (2006) A method for in situ estimation of prey selectivity and predation rate in
798 large plankton, exemplified with the jellyfish *Aurelia aurita* (L.). *J Exp Mar Bio Ecol*
799 328:113–126. doi: 10.1016/j.jembe.2005.07.002

800 Huang XG, Huang B, Zeng Y, Li SX (2015) Effect of dinoflagellates and diatoms on the
801 feeding response and survival of *Aurelia* sp. polyps. *Hydrobiologia* 754:179–188. doi:

802 10.1007/s10750-014-2023-1

803 Hubot N, Lucas CH, Piraino S (2017) Environmental control of asexual reproduction and
804 somatic growth of *Aurelia* spp. (Cnidaria, Scyphozoa) polyps from the Adriatic Sea.
805 PLoS One 12:e0178482. doi: 10.1371/journal.pone.0178482

806 Ikeda H, Mizota C, Uye S-I (2017) Bioenergetic characterization in *Aurelia aurita* (Cnidaria:
807 Scyphozoa) polyps and application to natural polyp populations. Mar Ecol Prog Ser
808 568:87–100. doi: 10.3354/meps12055

809 Ishii H, Båmstedt U (1998) Food regulation of growth and maturation in a natural population
810 of *Aurelia aurita* (L.). J Plankton Res 20:805–816. doi: 10.1093/plankt/20.5.805

811 Ishii H, Tanaka F (2001) Food and feeding of *Aurelia aurita* in Tokyo Bay with an analysis of
812 stomach contents and a measurement of digestion times. In: Purcell JE, Graham WM,
813 Dumont HJ (eds) Jellyfish Blooms: Ecological and Societal Importance. Developments
814 in Hydrobiology, vol 155, Springer Netherlands, Dordrecht, pp 311–320. doi:
815 10.1007/978-94-010-0722-1_26

816 Jackson AL, Inger R, Parnell AC, Bearhop S (2011) Comparing isotopic niche widths among
817 and within communities: SIBER - Stable Isotope Bayesian Ellipses in R. J Anim Ecol
818 80:595–602. doi: 10.1111/j.1365-2656.2011.01806.x

819 Jaïne AK (2010) Data clustering: 50 years beyond K-means Pattern Recognit Lett 31:651-
820 666. 10.1016/j.patrec.2009.09.011.

821 Javidpour J, Cipriano-Maack AN, Mittermayr A, Dierking J (2016) Temporal dietary shift in
822 jellyfish revealed by stable isotope analysis. Mar Biol 163:112. doi: 10.1007/s00227-
823 016-2892-0

824 Kamiyama T (2013) Planktonic ciliates as food for the scyphozoan *Aurelia aurita* (s.l.):
825 Effects on asexual reproduction of the polyp stage. J Exp Mar Bio Ecol 445:21–28. doi:
826 10.1016/j.jembe.2013.03.018

827 Kassambara A, Mundt F (2017) factoextra: Extract and Visualize the Results of Multivariate
828 Data Analyses. 1–74. R package version 1.0.5

829 Layman CA, Araujo MS, Boucek R, Hammerschlag-Peyer CM, Harrison E, Jud ZR, Matich
830 P, Rosenblatt AE, Vaudo JJ, Yeager LA, Post DM, Bearhop S (2012) Applying stable
831 isotopes to examine food-web structure: an overview of analytical tools. Biol Rev
832 87:545–562. doi: 10.1111/j.1469-185X.2011.00208.x

833 Lo WT, Chen IL (2008) Population succession and feeding of scyphomedusae, *Aurelia aurita*,
834 in a eutrophic tropical lagoon in Taiwan. Estuar Coast Shelf Sci 76:227–238. doi:
835 10.1016/j.ecss.2007.07.015

836 Lucas CH (1994) Biochemical composition of *Aurelia aurita* in relation to age and sexual
837 maturity. J Exp Mar Bio Ecol 183:179–192. doi: 10.1016/0022-0981(94)90086-8

838 Lucas CH (2001) Reproduction and life history strategies of the common jellyfish, *Aurelia*
839 *aurita*, in relation to its ambient environment. In: Purcell JE, Graham WM, Dumont HJ
840 (eds) Jellyfish Blooms: Ecological and Societal Importance. Developments in
841 Hydrobiology, vol 155, Springer Netherlands, Dordrecht, pp 229–246doi: 10.1007/978-
842 94-010-0722-1_19

843 Lucas CH, Hirst AG, Williams JA (1997) Plankton Dynamics and *Aurelia aurita* Production
844 in Two Contrasting Ecosystems: Comparisons and Consequences. Estuar Coast Shelf Sci
845 45:209–219. doi: 10.1006/ecss.1996.0173

846 Marques R, Cantou M, Soriano S, Molinero J-C, Bonnet D (2015a) Mapping distribution and
847 habitats of *Aurelia* sp. polyps in Thau lagoon, north-western Mediterranean sea (France).
848 Mar Biol 162:1441–1449. doi: 10.1007/s00227-015-2680-2

849 Marques R, Albouy-Boyer S, Delpy F, Carré C, Le Floc'H É, Roques C, Molinero J-C,
850 Bonnet D (2015b) Pelagic population dynamics of *Aurelia* sp. in French Mediterranean
851 lagoons. J Plankton Res 37:1019–1035. doi: 10.1093/plankt/fbv059

852 Marques R, Darnaude AM, Schiariti A, Tremblay Y, Molinero J-C, Soriano S, Hatey E,
853 Colantoni S, Bonnet D (2019) Dynamics and asexual reproduction of the jellyfish
854 *Aurelia coerulea* benthic life stage in the Thau lagoon (northwestern Mediterranean).
855 Mar Biol 166:74. doi: 10.1007/s00227-019-3522-4

856 Martinez Arbizu P (2019) pairwiseAdonis: Pairwise multilevel comparison using adonis. R
857 package, version 0.0.1.

858 Martinussen MB, Båmstedt U (2001) Digestion rate in relation to temperature of two
859 gelatinous planktonic predators. Sarsia 86:21–35. doi:
860 10.1080/00364827.2001.10420458

861 Milisenda G, Rossi S, Vizzini S, Fuentes VL, Purcell JE, Tilves U, Piraino S (2018) Seasonal
862 variability of diet and trophic level of the gelatinous predator *Pelagia noctiluca*
863 (Scyphozoa). Sci Rep 8:12140. doi: 10.1038/s41598-018-30474-x

864 Millet B, Cecchi P (1992) Wind-induced hydrodynamic control of the phytoplankton biomass
865 in a lagoon ecosystem. Limnol Oceanogr 37:140–146. doi: 10.4319/lo.1992.37.1.0140

866 Mills C (2001) Are population increasing globally in response to changing ocean conditions?
867 Hydrobiologia 451:55–68. doi: <https://doi.org/10.1023/A:1011888006302>

868 Mongrue R, Vanhoutte-Brunier A, Fiandrino A, Valette F, Ballé-Béganton J, Pérez Agúndez
869 JA, Gallai N, Derolez V, Roussel S, Lample M, Laugier T (2013) Why, how, and how
870 far should microbiological contamination in a coastal zone be mitigated? An application
871 of the systems approach to the Thau lagoon (France). J Environ Manage 118:55–71. doi:
872 10.1016/j.jenvman.2012.12.038

873 Morais P, Dias E, Cruz J, Chainho P, Angélico MM, Costa JL, Barbosa AB, Teodósio MA
874 (2017) Allochthonous-derived organic matter subsidizes the food sources of estuarine
875 jellyfish. J Plankton Res 39:870–877. doi: 10.1093/plankt/fbx049

876 Nixon SW (1995) Coastal marine eutrophication: A definition, social causes, and future

877 concerns. *Ophelia* 41:199–219. doi: 10.1080/00785236.1995.10422044

878 Oksanen J, Blanchet FG, Friendly M, Kindt R, Legendre P, Mcglinn D, Minchin PR, O’Hara
879 RB, Simpson GL, Solymos P, Stevens MHH, Szoecs E, Wagner H (2019) Vegan:
880 Community Ecology Package. R package, version 2.5-4

881 Östman C (1997) Abundance, feeding behaviour and nematocysts of scyphopolyps (Cnidaria)
882 and nematocysts in their predator, the nudibranch *Coryphella verrucosa* (Mollusca). In:
883 Naumov AD, Hummel H, Sukhotin AA, Ryland JS (eds) Interactions and Adaptation
884 Strategies of Marine Organisms. Springer Netherlands, Dordrecht, pp 21–28

885 Pernet F, Malet N, Pastoureaud A, Vaquer A, Quéré C, Dubroca L (2012) Marine diatoms
886 sustain growth of bivalves in a Mediterranean lagoon. *J Sea Res* 68:20–32. doi:
887 10.1016/j.seares.2011.11.004

888 Perrin J-L, Tournoud M-G (2009) Hydrological processes controlling flow generation in a
889 small Mediterranean catchment under karstic influence. *Hydrol Sci J* 54:1125–1140. doi:
890 10.1623/hysj.54.6.1125

891 Pinnegar JK, Polunin NVC (1999) Differential fractionation of $\delta^{13}\text{C}$ and $\delta^{15}\text{N}$ among fish
892 tissues: implications for the study of trophic interactions. *Funct Ecol* 13:225–231. doi:
893 10.1046/j.1365-2435.1999.00301.x

894 Pitt KA, Connolly RM, Meziane T (2009) Stable isotope and fatty acid tracers in energy and
895 nutrient studies of jellyfish: A review. *Hydrobiologia* 616:119–132. doi:
896 10.1007/s10750-008-9581-z

897 Plus M, La Jeunesse I, Bouraoui F, Zaldívar J-M, Chapelle A, Lazure P (2006) Modelling
898 water discharges and nitrogen inputs into a Mediterranean lagoon: Impact on the primary
899 production. *Ecological Modelling* 193:69–89. doi:10.1016/j.ecolmodel.2005.07.037

900 Post DM (2002) Using stable isotopes to estimate trophic position: models, methos, and
901 assumptions. *Ecology* 83:703–718. doi: Doi 10.2307/3071875

902 Post DM, Layman CA, Arrington DA, Takimoto G, Quattrochi J, Montaña CG (2007) Getting
903 to the fat of the matter: Models, methods and assumptions for dealing with lipids in
904 stable isotope analyses. *Oecologia* 152:179–189. doi: 10.1007/s00442-006-0630-x

905 Purcell JE (2012) Jellyfish and Ctenophore Blooms Coincide with Human Proliferations and
906 Environmental Perturbations. *Ann Rev Mar Sci* 4:209–235. doi: 10.1146/annurev-
907 marine-120709-142751

908 Rassoulzadegan F, Sheldon RW (1986) Predator-prey interactions of nanozooplankton and
909 bacteria in an oligotrophic marine environment. *Limnol Oceanogr* 31:1010–1029. doi:
910 10.4319/lo.1986.31.5.1010

911 Stock BC, Semmens BX (2016) MixSIAR GUI User Manual. Version 3.1 1–42. doi:
912 10.5281/zenodo.47719

913 Syväranta J, Rautio M (2010) Zooplankton, lipids and stable isotopes: importance of seasonal,
914 latitudinal, and taxonomic differences. *Can J Fish Aquat Sci* 67:1721–1729. doi:
915 10.1139/F10-091

916 Turk V, Lučić D, Flander-Putrlje V, Malej A (2008) Feeding of *Aurelia* sp. (Scyphozoa) and
917 links to the microbial food web. *Mar Ecol* 29:495–505. doi: 10.1111/j.1439-
918 0485.2008.00250.x

919 Utermöhl H (1958) Zur Vervollkommnung der quantitativen Phytoplankton-Methodik. *SIL*
920 *Commun* 1953-1996 9:1–38. doi: 10.1080/05384680.1958.11904091

921 Wang Y-T, Zheng S, Sun S, Zhang F (2015) Effect of temperature and food type on asexual
922 reproduction in *Aurelia* sp.1 polyps. *Hydrobiologia* 754:169–178. doi: 10.1007/s10750-
923 014-2020-4

924 Yokoyama H, Tamaki A, Harada K, Shimoda K, Koyama K, Ishihi Y (2005) Variability of
925 diet-tissue isotopic fractionation in estuarine macrobenthos. *Mar Ecol Prog Ser* 296:115–
926 128. doi: 10.3354/meps296115

927 Vander Zanden MJ, Rasmussen JB (2001) Variation in $\delta^{15}\text{N}$ and $\delta^{13}\text{C}$ trophic fractionation:
928 Implications for aquatic food web studies. *Limnol Oceanogr* 46:2061–2066. doi:
929 10.4319/lo.2001.46.8.2061

930 Zheng S, Sun X, Wang Y, Sun S (2015) Significance of different microalgal species for
931 growth of moon jellyfish ephyrae, *Aurelia* sp.1. *J Ocean Univ China* 14:823–828. doi:
932 10.1007/s11802-015-2775-x

933 Zuur AF, Ieno EN, Walker NJ, Saveliev AA, Smith GM (2009) *Mixed Effects Models and*
934 *Extensions in Ecology with R*. Springer New York

935

936

937

938

939

940 **Acknowledgment:**

941 We would like to thank Solenn Soriano, Nicolas Nouguier, and Remy Valdes for their
942 technical support during SCUBA dives and fieldwork. We also thank Sandrine Crochemore
943 and Sébastien Colantoni for their assistance during laboratory samples preparation. We thank
944 Simon Julien from *huitres-bouzigues.com* for providing the cultivated oyster samples.
945 Plankton diversity and abundance data are part of a long-term monitoring program on
946 microbial communities in the Thau lagoon funded by *Observatoire des Sciences de l'Univers*
947 *OREME* (OSU-OREME). Data are available on
948 (https://data.oreme.org/plankton/plankton_thau_home). The laboratory analysis of samples to
949 determine stable isotope signatures was performed at the Stable Isotope Facility at the
950 University of California, Davis, USA. The authors declare that they have no conflict of
951 interests.

952 **Tables**

953 Table 1: Frequency of occurrence (FO), index of relative importance (IRI) and mean
 954 abundance of prey items found in *A. coerulea* medusae gut contents during the period of its
 955 presence in the Thau lagoon. Numbers in parenthesis are the number of medusae with prey
 956 items analyzed.

Prey	FO (%)			IRI (%)			Abundance (\pm SD) (ind.medusae ⁻¹)		
	Apr (5)	May (9)	Jun (8)	Apr (5)	May (9)	Jun (8)	Apr (5)	May (9)	Jun (8)
Phytoplankton	20.0	33.3	0.0	3.4	5.6	0.0	1.0 (2.2)	1.0 (1.8)	0.0 (0.0)
Microzooplankton	60.0	55.6	0.0	7.5	12.5	0.0	2.2 (3.8)	2.2 (3.4)	0.0 (0.0)
Mesozooplankton (total)	80.0	88.9	100	89.1	81.9	100	26.2 (35.4)	14.6 (13.4)	10.3 (18.3)
- <i>Copepods</i>	40.0	66.7	87.5	34.7	21.9	46.3	10.2 (20.1)	3.9 (5.7)	4.8 (9.9)
- <i>Nauplii (copepods and cirripeds)</i>	60.0	88.9	62.5	4.8	31.3	41.5	1.4 (2.1)	5.6 (8.5)	4.3 (7.8)
- <i>Other crustaceans</i>	20.0	55.6	50.0	0.7	10.0	8.5	0.2 (0.4)	1.8 (3.5)	0.9 (1.1)
- <i>Non-crustaceans</i>	60.0	66.7	25.0	49.0	18.8	3.7	14.4 (20.9)	3.3 (4.5)	0.4 (0.7)

957

958

959 Table 2: Parameters of the generalized linear models used to assess correlations between the
 960 benthic population dynamics variables (scyphistomae coverage and scyphistomae producing
 961 buds) with the abundance $[\ln(x+1)]$ of phytoplankton (cell L⁻¹), microzooplankton (cell L⁻¹)
 962 and mesozooplankton (ind m⁻³).

	Estimate	Std. Error	t value	p-value
Scyphistomae coverage (%)				
(Intercept)	-0.17	0.07	-2.46	0.03
Phytoplankton	0.02	0.01	2.97	0.01
Microzooplankton	0.01	0.01	2.10	0.05
Mesozooplankton	0.00	0.00	0.02	0.98
Scyphistomae producing buds (%)				
(Intercept)	-3.82	0.35	-10.95	< 0.01
Phytoplankton	-0.01	0.03	-0.47	0.64
Microzooplankton	0.26	0.03	10.19	< 0.01
Mesozooplankton	0.00	0.02	-0.09	0.93

963

964

965 Table 3: Stable $\delta^{13}\text{C}$ and $\delta^{15}\text{N}$ isotope signatures (mean \pm SD) of *A. coerulea* and organic
 966 matter sources used in MixSIAR model for each isotopic niche period. Sources A are the
 967 values of organic matter sources used for scyphistomae models, including all data, while
 968 Sources B are the values of organic matter sources collected from February to May, used for
 969 medusae models. *n* is the number of samples used to calculate each mean. SP: small plankton;
 970 Mesoz.: mesozooplankton; SOM: sedimentary organic matter.

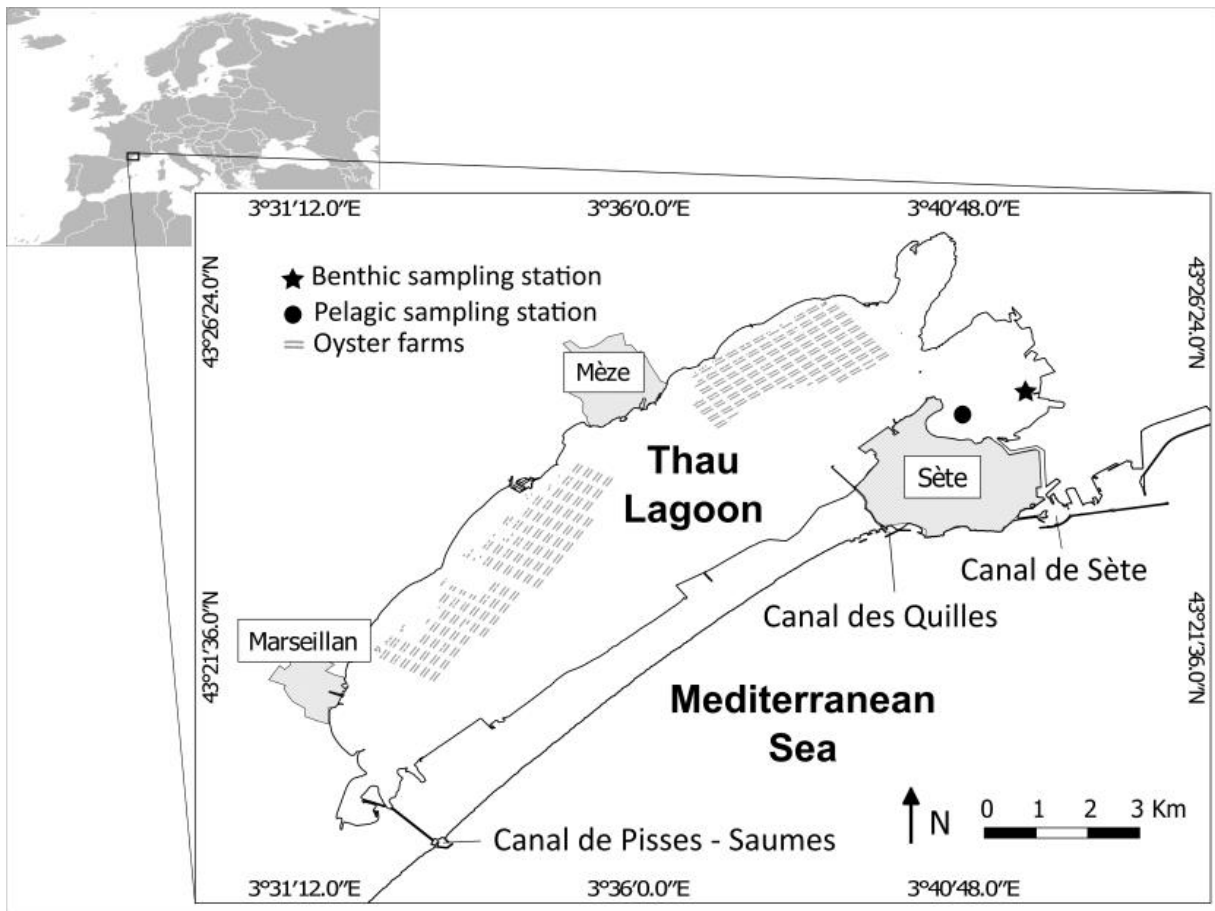
	Period 1			Period 2			Period 3		
	$\delta^{13}\text{C}$ (\pm SD) ‰	$\delta^{15}\text{N}$ (\pm SD) ‰	<i>n</i>	$\delta^{13}\text{C}$ (\pm SD) ‰	$\delta^{15}\text{N}$ (\pm SD) ‰	<i>n</i>	$\delta^{13}\text{C}$ (\pm SD) ‰	$\delta^{15}\text{N}$ (\pm SD) ‰	<i>n</i>
Scyphistomae	-22.8 (0.4)	8.0 (0.5)	18	-19.3 (0.2)	9.0 (0.1)	9	-21.1 (0.3)	8.5 (0.4)	9
Medusae	-23.4 (0.7)	8.1 (0.3)	13	-19.4 (0.5)	8.9 (0.3)	7			
Sources A									
SP	-22.1 (2.0)	6.5 (0.3)	18	-20.6 (0.8)	6.2 (0.7)	22	-21.0 (0.9)	6.7 (0.3)	6
Mesoz.	-22.9 (0.9)	8.0 (0.4)	9	-19.2 (0.7)	7.4 (0.3)	12	-20.1 (0.1)	7.5 (0.0)	3
SOM	-20.2 (0.9)	5.5 (0.3)	6	-20.6 (0.1)	5.4 (0.2)	6	-20.7 (0.0)	5.3 (0.0)	2
Sources B									
SP	-23.3 (0.9)	6.4 (0.3)	12	-20.9 (0.5)	5.8 (0.3)	15			
Mesoz.	-23.4 (0.3)	8.2 (0.2)	6	-18.8 (0.2)	7.3 (0.3)	9			
SOM	-18.9 (0.0)	5.8 (0.1)	2	-20.5 (0.0)	5.6 (0.0)	2			

971

972

973 **Figures**

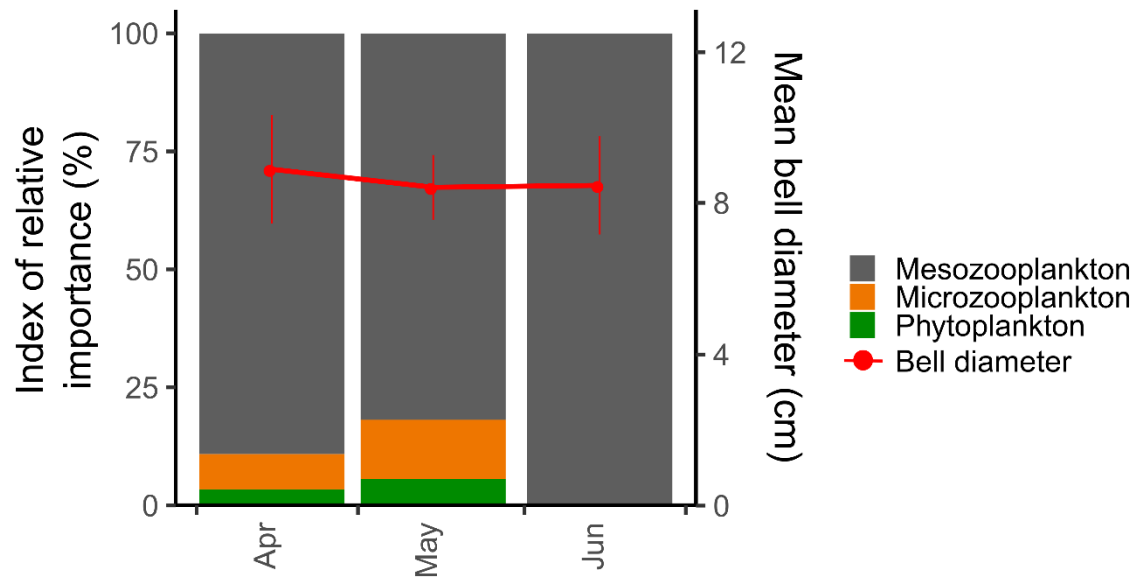
974



975

976 Fig. 1: Map of the Thau lagoon showing the location of the benthic (star) and pelagic (dot)
977 sampling stations for this study. Shaded areas represent urban zones and grey points represent
978 oyster farms.

979



980

981 Fig. 2: Index of relative importance of the three main prey groups found in the guts of *A.*

982 *coerulea* medusae and the bell diameter of all individuals collected for gut content analysis.

983

984

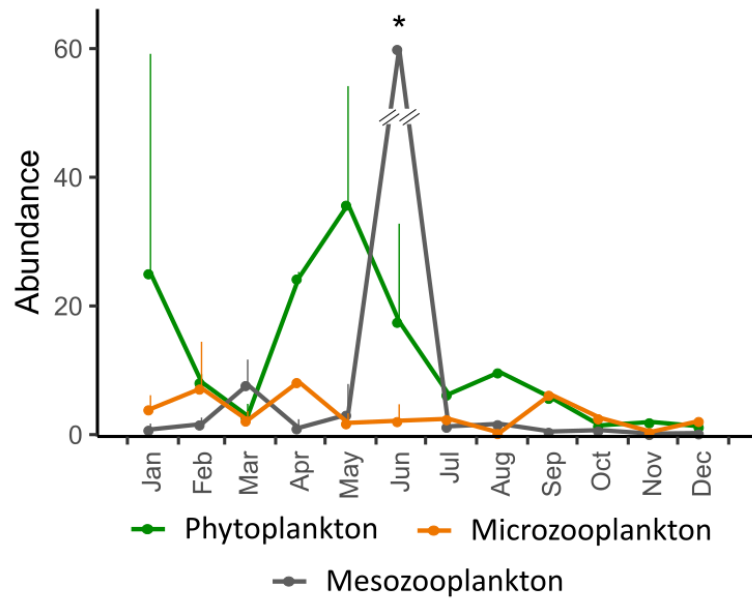
985

986

987

988

989



990

991 Fig. 3: Temporal variability of phytoplankton ($\times 10^3$ cell L⁻¹), microzooplankton ($\times 10^3$ cell L⁻¹), and mesozooplankton ($\times 10^3$ ind m⁻³) abundance collected in the Thau lagoon during the
 992 study period. All values represent monthly mean \pm SD. In June 2017 (*), the mean (\pm SD) of
 993 mesozooplankton abundance was $90,895 \pm 107,072$ ind m⁻³.
 994

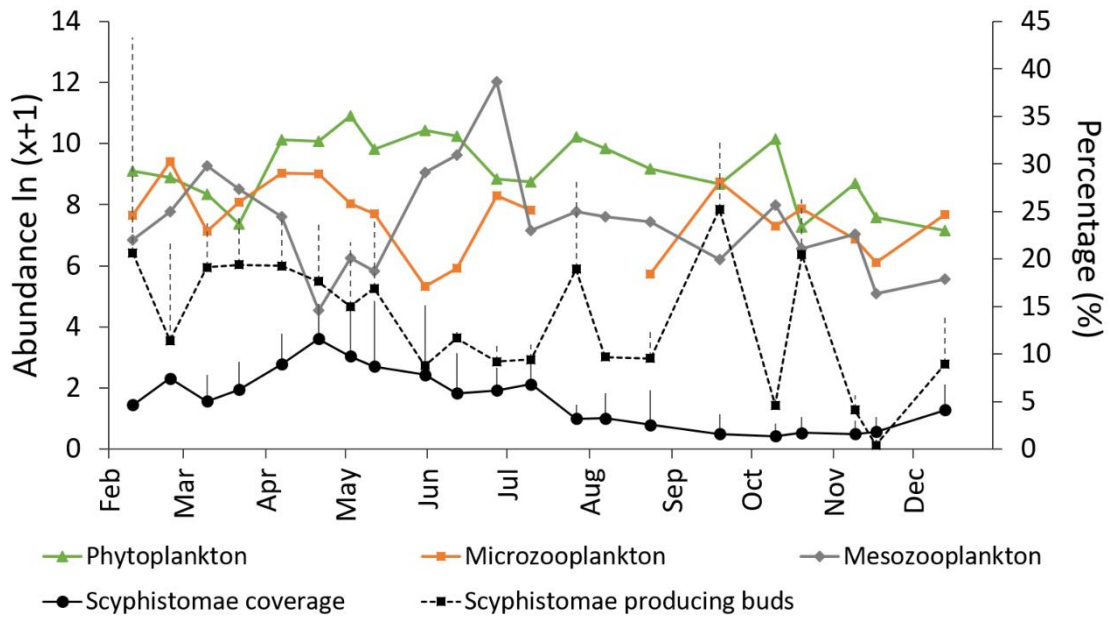
995

996

997

998

999

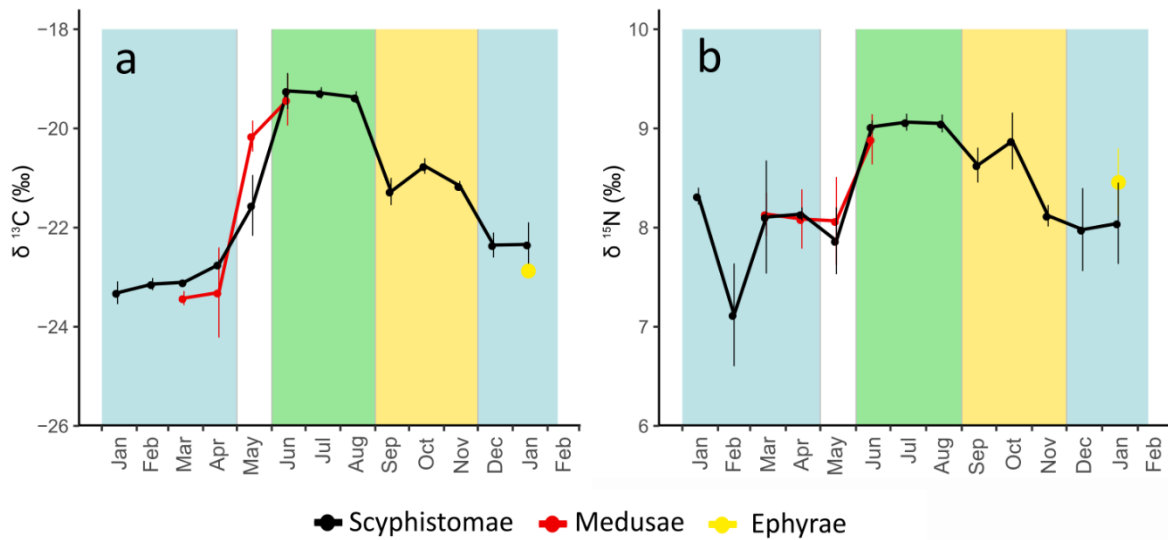


1000

1001 Fig. 4: Temporal variability of the *A. coerulea* benthic population dynamics and the
 1002 abundance of plankton in the Thau lagoon during the study period (adapted from Marques et
 1003 al. 2019). Black lines represent the percentage of scyphistomae coverage (i.e., an indicator of
 1004 population size) and the percentage of the scyphistomae producing buds. Each point
 1005 represents replicate means and vertical lines are SD (see Marques et al 2019 for further
 1006 information). Coloured lines represent the non-averaged abundance (after logarithmic
 1007 transformation) of phytoplankton (cell L^{-1}), microzooplankton (cell L^{-1}), and
 1008 mesozooplankton (ind m^{-3}).

1009

1010



1011

1012 Fig. 5: Temporal variability of $\delta^{13}\text{C}$ (a) and $\delta^{15}\text{N}$ (b) of *A. coerulea* scyphistomae, medusae,
 1013 and ephyrae in Thau. All values represent monthly means \pm SD. Background colours
 1014 represent the different isotopic niche periods (periods 1, 2, and 3 in blue, green, and yellow,
 1015 respectively; see Fig.6). May represents a transitional period and it was not included in any
 1016 isotopic niche period.

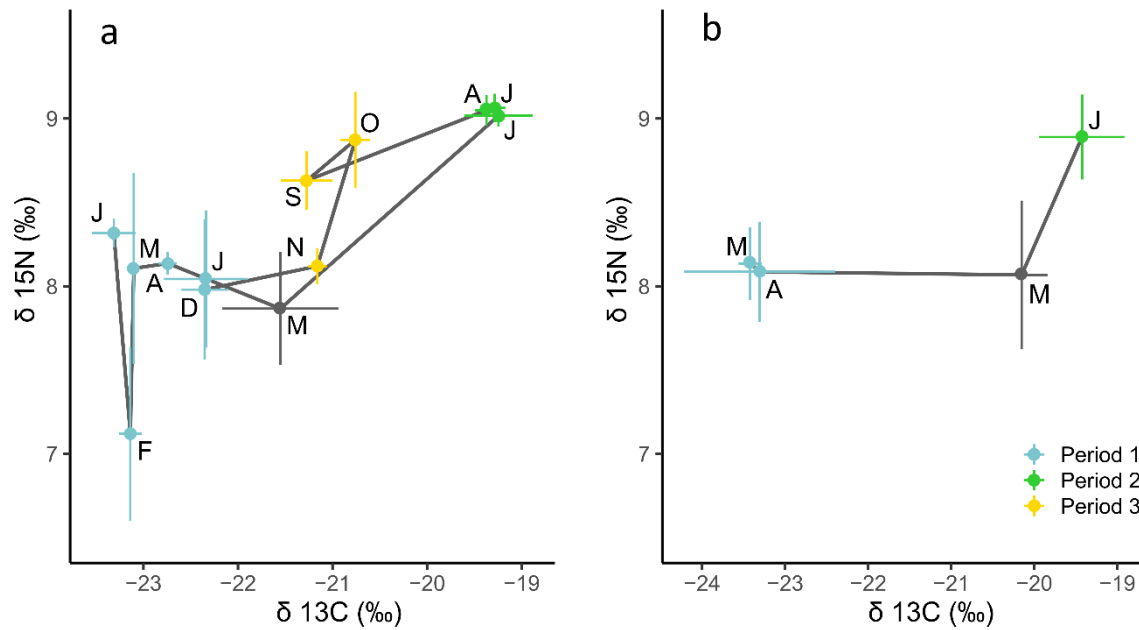
1017

1018

1019

1020

1021

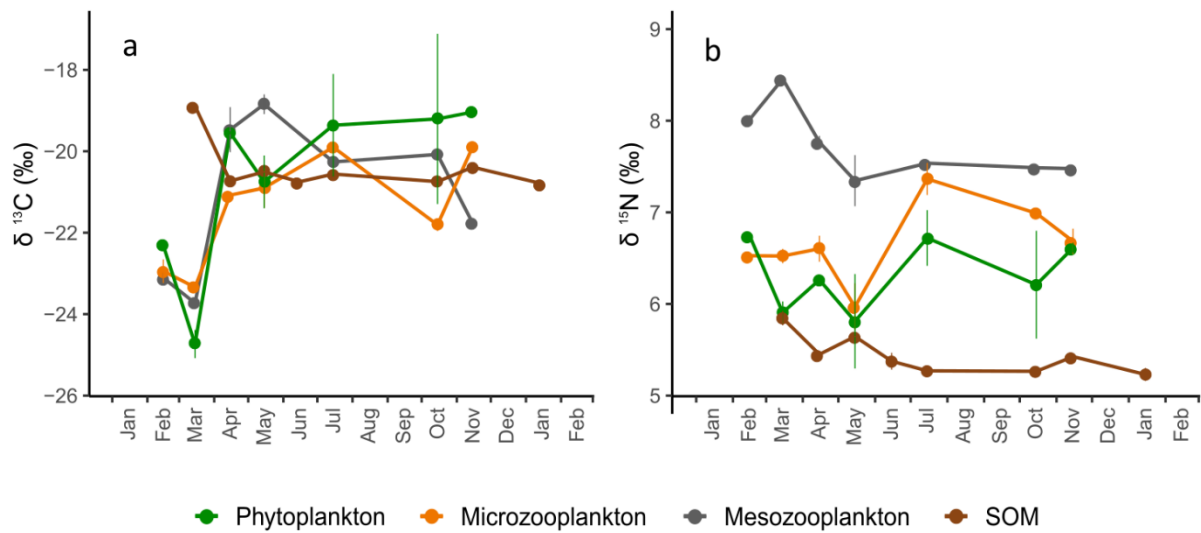


1022

1023 Fig. 6: Time trajectory of the evolution of the isotope signature, averaged by month, from *A.*
 1024 *coerulea* scyphistomae (a) and medusae (b). Letters represent months (from January 2017 to
 1025 January 2018). Coloured points represent isotopic niche periods defined after cluster analysis:
 1026 period 1 is from January to April 2017 and from December 2017 to January 2018; period 2 is
 1027 from June to August 2017 and period 3 is from September to November 2017. May represents
 1028 the transition between periods 1 and 2 and was therefore not included in any isotopic niche
 1029 period.

1030

1031



1032

1033 Fig. 7: Monthly variability of the $\delta^{13}\text{C}$ (a) and $\delta^{15}\text{N}$ (b) of the organic matter sources collected

1034 in this study. SOM: sedimentary organic matter.

1035

1036

1037

1038

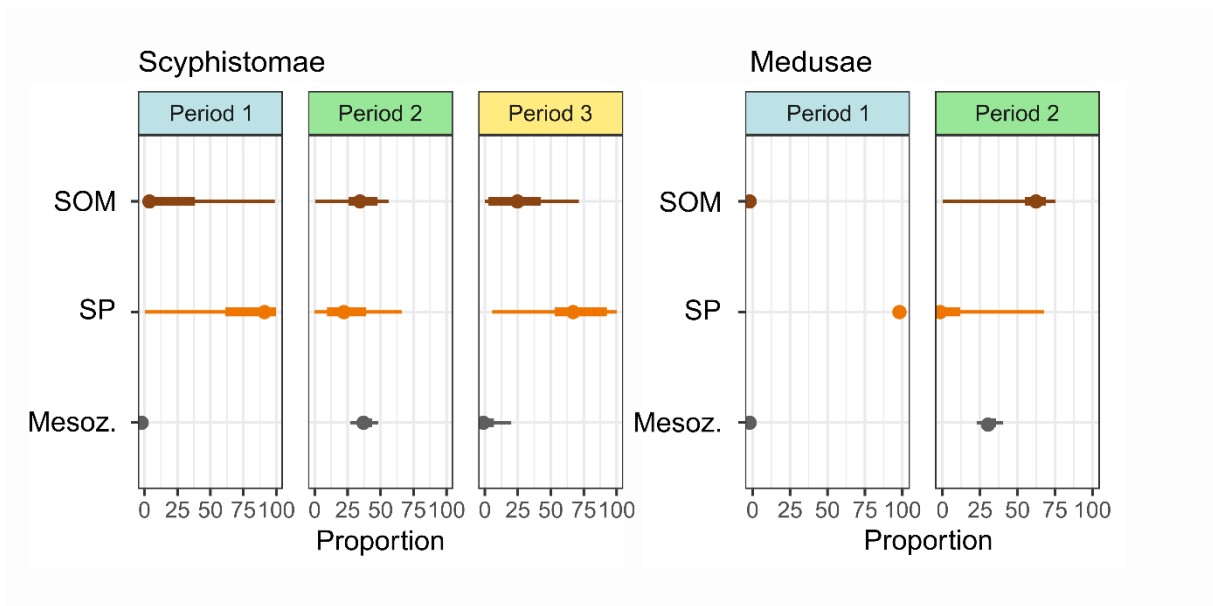
1039

1040

1041

1042

1043

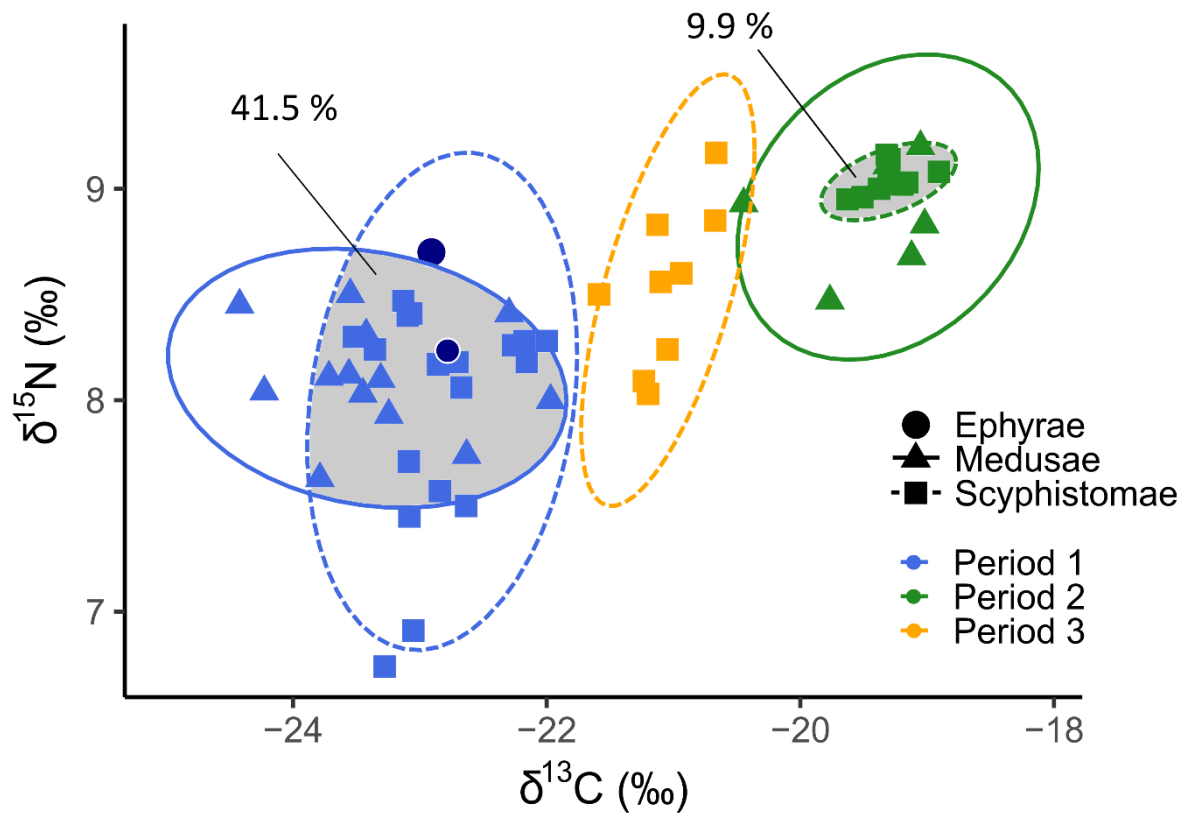


1044

1045 Fig. 8: Proportion of the contribution of each organic matter source to the diet of *A. coerulea*
 1046 scyphistomae and medusae during the different isotopic niche periods. The proportion was
 1047 calculated using MixSIAR mixing models. The points indicate the median and the horizontal
 1048 bars represent 75% and 95% Bayesian credibility intervals. SOM: sedimentary organic matter,
 1049 SP: small plankton, Mesoz.: mesozooplankton.

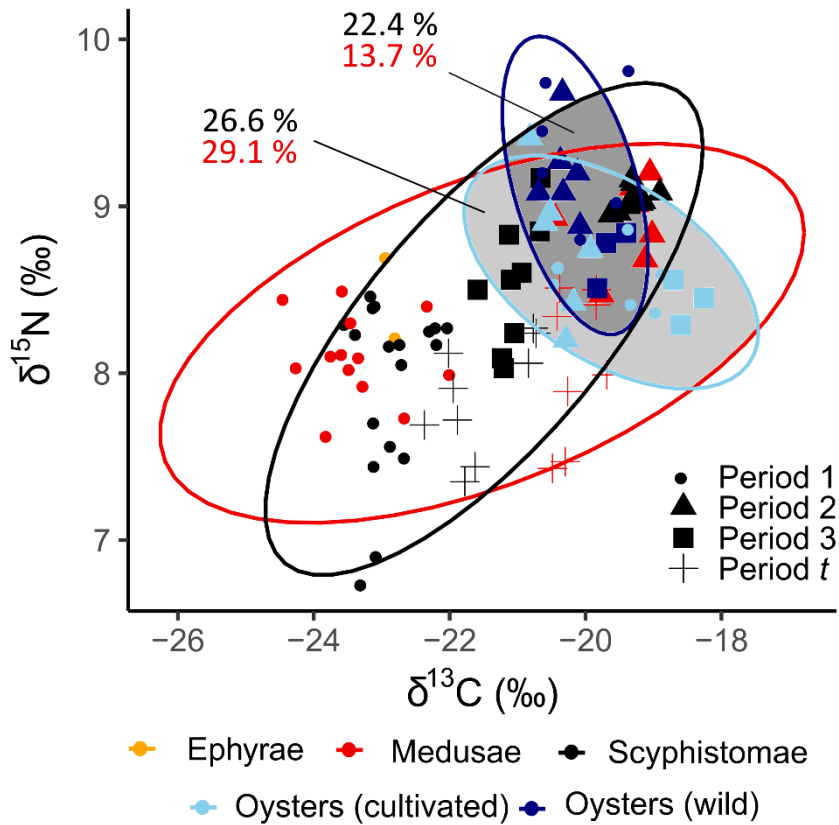
1050

1051



1052

1053 Fig. 9: Biplot of isotope values of *A. coerulea* ephyrae, medusae, and scyphistomae. Ellipses
 1054 indicate their isotopic niche in the Thau lagoon (as 95% confidence ellipse of the bivariate
 1055 means), during the different isotopic niche periods. Grey areas and associated values indicate
 1056 the percentage of overlap, when observed.



1057

1058 Fig. 10: Biplot of isotope values of *A. coerulea* ephyrae, medusae, scyphistomae, and oysters

1059 (*C. gigas*). Ellipses indicate their isotopic niche in the Thau lagoon, considering the whole

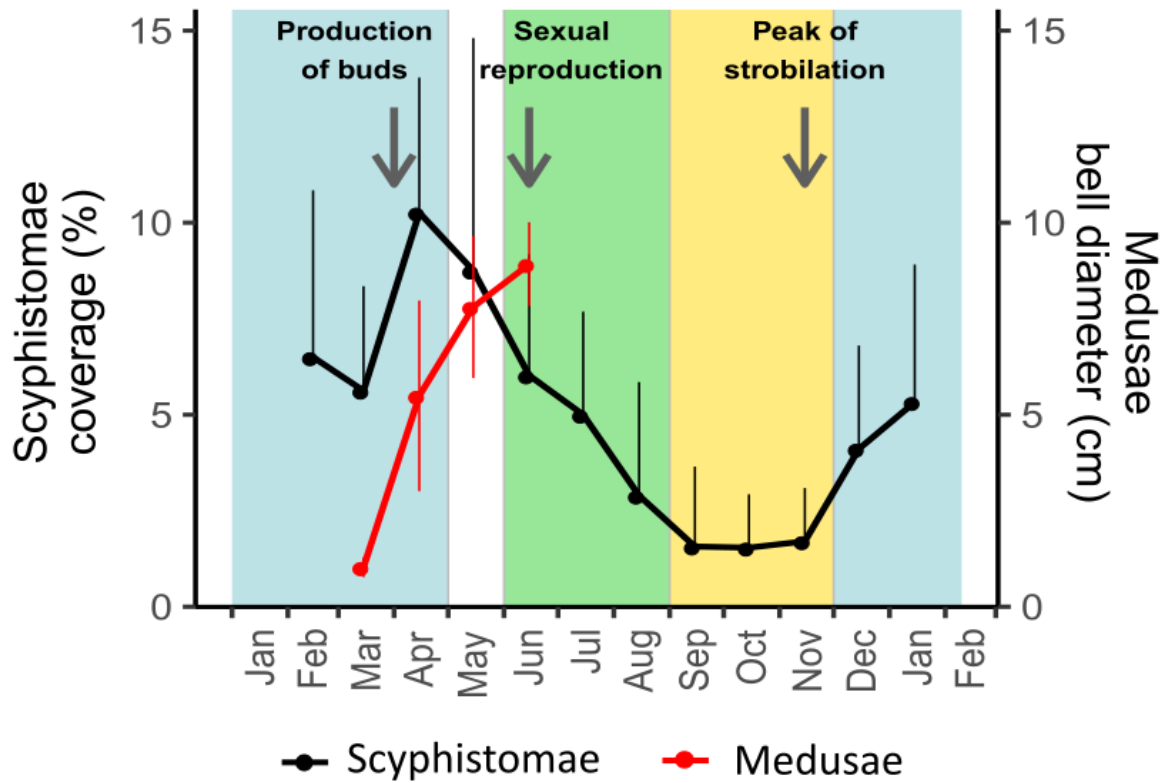
1060 study period (as 95% confidence ellipse of the bivariate means). Dark and light grey areas

1061 indicate niche overlap between *A. coerulea* and wild or cultivated oysters, respectively.

1062 Associated values on the graph indicate the percentage of overlap with medusae (in red) and

1063 scyphistomae (in black). The shape of points represents isotopic niche periods (period *t*:

1064 transitional period, i.e., samples collected in May).



1065

1066 Fig. 6: Scyphistomae coverage (in black, from Marques et al. 2019) and medusae bell
 1067 diameter of the individuals collected for stable isotope analysis in this study (in red). The
 1068 arrows indicate the main periods of sexual and asexual reproduction of *A. coerulea* (after
 1069 Marques et al. 2015b, 2019). The background colours represent the isotopic niche periods
 1070 (periods 1, 2, and 3 in blue, green, and yellow, respectively).

1071